Structural Evolution of Salt-Influenced Fold-and-Thrust belts: A Synthesis and New Insights From Basins Containing Isolated Salt Diapirs

Oliver B. Duffy[1*], Tim P. Dooley[1], Michael R. Hudec[1], Martin P.A. Jackson[1], Naiara Fernandez[1], Christopher A-L. Jackson[2], Juan I. Soto[3]

[1]Bureau of Economic Geology, Jackson School of Geosciences, The University of Texas at Austin, University Station, Box X, Austin, Texas, 78713-8924, USA

[2]Basins Research Group (BRG), Department of Earth Science & Engineering, Imperial College, Prince Consort Road, London, United Kingdom, SW7 2BP

[3]Departamento de Geodinamica and Instituto Andaluz de Ciencias de la Tierra (CSIC-UGR), Universidad de Granada, Campus Fuentenueva, 18071-Granada, Spain

** Corresponding Author: oliver.duffy@beg.utexas.edu*

Running Title: Shortening of Isolated-Diapir Provinces

Keywords: salt tectonics; shortening; fold-and-thrust belts; diapirs; minibasins; Zagros, Gulf of Mexico

Abstract

Lateral shortening is expressed in unique ways in salt basins, especially if pre-shortening diapirs are present. We present an overview and new 3-D conceptual models capturing the evolution of shortening structures formed in salt provinces dominated by precursor isolated diapirs (termed *isolated-diapir provinces*). In such provinces, isolated diapirs form only a minor volumetric component of a sedimentary basin, however, due to the relative weakness of rock salt and their ability to localize strain, during shortening they have a disproportionately large influence on structural development.

We find three key mechanical principles govern the processes and structural styles developed during shortening of isolated-diapir provinces. First, salt diapirs shorten before surrounding sedimentary rocks due to their relative weakness, and so form salients in the thrust front during early shortening. Second, diapirs tend to nucleate folds and faults, which radiate out from the diapirs. Third, as diapir walls converge, the roof must shorten. Extrusive salt sheets are expelled through thin roofs, but thicker roofs resist piercement and so tend to undergo complex folding and faulting.

As a result of these principles, the first-order controls on the structural styles expressed across a shortened isolated-diapir province are the pre-shortening configuration of diapirs, the connectivity of the diapirs prior to shortening, total strain magnitude, and diapir roof thickness. Second-order controls include the initial cross-sectional and map-view geometry of diapirs, diapir size, and diapir orientation with respect to the shortening direction.

1. Introduction

The geometry and kinematics of fold-and-thrust belts are generally well understood as a result of their spectacular exposure in mountain ranges around the world (e.g., Bally et al., 1966; Dahlstrom, 1969; Boyer and Elliott, 1982). A relatively poorly-understood aspect of these systems involves fold-and-thrust belts that detach on, and are influenced by mobile salt. In these settings 3-D shortening styles can be particularly complex and diverse due to: i) salt being much weaker than local sedimentary rocks, creating a strength anisotropy during shortening; and ii) the ability of salt to flow and thus be heterogeneously distributed prior to the onset of shortening (e.g. Davis and Engelder, 1985; Letouzey et al., 1995). Thus, the configuration of salt prior to shortening exerts a major control on salt-detached structural styles, with three styles standing out.

In the first and simplest case, bedded salt is undeformed, forming a continuous gently-dipping layer prior to shortening. In this situation, where shortening occurs with no precursor salt structures present, the salt simply acts as a décollement, 'lubricating' predominantly linear fold-and-thrust belts above that show extremely low taper angles (e.g. Davis and Engelder, 1985; Letouzey et al., 1995; Morley et al., 2011) (Fig. 1a). Common structural styles observed in such settings are salt-bearing thrusts, box folds, and long-wavelength, broad anticlines separated by narrow, sharp synclines (Fig. 1a). In general, there is little along-strike variability in structural style, aside from those developed due to along-strike variations in the depositional thickness of the salt (e.g. Davis and Engelder, 1985). Contractional provinces in which salt acts primarily as a detachment include the Valley and Ridge Province of the Appalachians (e.g. Frey, 1973), the Betics and Rif (e.g., Flinch and Soto, 2017), the Pyrenees (e.g., Canerot et al., 2005; Roca et al.,

2011; Carlola et al., 2015; Cámara and Flinch, 2017), the Albanides (Velaj et al., 1999; Bega and Soto, 2017), the Carpathians and Balkans (e.g., Georgiev and Tari, 2017), the Jura Mountains and the Alps (e.g., Guellec et al., 1990; Sommaruga et al., 2017; Leitner and Spötl, 2017), the Salt Range (e.g. Grelaud et al., 2002), the Rhodanian Basin (Lickorish and Ford, 1998), the Perdido fold belt in the Northwestern Gulf of Mexico (e.g. Trudgill et al., 1999), and the Northwestern Zagros Mountains (e.g. Sherkati et al., 2006; Dooley et al., 2007).

In the second and third styles, which are less understood, diapirs exist prior to shortening. During shortening, the weak diapirs narrow and rise, whereas the relatively strong surrounding sedimentary rocks remain largely undeformed (e.g. Nilsen et al, 1995; Canerot et al. 2005; Rowan and Vendeville, 2006; Callot et al., 2007; Hudec et al, 2011; Bega and Soto, 2017; Duffy et al, 2017) (Fig 1b). Diapir provinces thus form sensitive barometers to lateral compressive stresses (Roca et al., 2006; Dooley et al., 2009; Hudec et al. 2011; Dooley et al., 2015). The style of shortening in these systems, and the characteristics of the resultant fold-and-thrust belts, depends to a large extent upon the pre-shortening configuration of the diapirs. Structural styles are also more prone to vary along the strike of the resultant fold-and-thrust belt.

In the second style, the focus of this study, isolated stocks or walls are encased in a relatively rigid sediment body (Fig. 2). We term this an *isolated-diapir province*. In the third style, not addressed in this study, isolated minibasins are surrounded by salt walls on all sides; that is, the minibasins are adrift in a 'sea of salt'. This third style was previously referred to as a *wall and basin* province in Harrison and Jackson (2014) and Kergaravat et al. (2016), but is herein termed an *isolated-minibasin province*. Isolated-diapir and isolated-minibasin provinces shorten differently due to differences in the volume and distribution of mechanically weak salt, as well as differences in the potential lateral mobility of minibasins (Duffy et al., 2017).

92 Here we focus on thin-skinned shortening of isolated-diapir provinces and on the
93 characteristics of the resultant fold-and-thrust belt. We outline the fundamental mechanical
94 principles that govern how isolated-diapir provinces shorten and use these principles to answer
95 the following questions: i) what structural styles develop as a single isolated diapir shortens? ii)
96 how do isolated diapirs interact with one another during shortening?; iii) how do pre-shortening
97 configuration, roof thickness and shortening magnitude control the structural styles developed
98 during shortening of isolated-diapir provinces?; and iv) how and why do structural styles vary
99 across an array? To answer these questions, we synthesize observations from natural examples
100 and physical models of shortened isolated-diapir provinces in what is, at present, a scattered
101 literature. The physical models are of particular value as key structural styles can be viewed in
102 any orientation, structural styles can be documented through time, and variables such as roof
103 thickness, shortening magnitude and diapir configuration may be modified. Based on our
104 observations we then develop a series of 3-D conceptual models that provide a template for
105 understanding the likely pre-shortening configuration, degree of shortening, and overall tectonic
106 history of isolated-diapir provinces. We provide examples of key features from shortened
107 isolated-diapir provinces such as the Fars Region of the Zagros Mountains in Iran (e.g. Callot et
108 al., 2012) and the Astrid Fold Belt in the Lower Congo Basin of Offshore Gabon (Jackson et al.,
109 2008) before highlighting differences between fold-and thrust belts developed in sedimentary
110 basins with and without precursor salt diapirs.
111 This study is based on observations from moderate- to mildly-shortened settings and physical
112 models. However, the pre-shortening diapir configurations and structural styles described here
113 may be applicable to earlier stages in highly-shortened orogenic settings where the earlier

structure in hard to decipher. Our work may also help enhance the validity of structural restorations and basin models in salt basins worldwide.

2. Mechanical Principles Governing the Styles Developed During Shortening of Isolated Diapirs

The structural style of a shortened isolated diapir is controlled largely by the difference in the mechanical strength between the relatively weak diapir and strong sedimentary rocks surrounding it (e.g. Nilsen et al, 1995; Roca et al., 2006; Rowan and Vendeville, 2006; Callot et al., 2007; Dooley et al., 2009; 2015). This difference in mechanical strength influences how diapirs shorten in three ways. First, shortening strain is preferentially focused on the diapir rather than the surrounding sedimentary rocks, thus the diapir deforms earlier and to a higher degree than the surrounding sedimentary rocks (e.g. Nilsen et al., 1995). Second, shortening structures nucleate at the diapir and propagate outwards into the surrounding sedimentary rocks (e.g. Callot et al., 2007; 2012; Jackson et al., 2008; Dooley et al 2009; 2015). Third, when the walls of the diapir converge, the roof also shortens (Nilsen et al, 1995; Dooley et al., 2009; 2015).

We first explore how single and geometrically-simple isolated diapirs respond to shortening before exploring the effects of more geometrically-complicated diapirs, diapir arrays, and variable roof thickness. Despite the complexity inherent in some diapir settings, it is critical to note that the three fundamental principles outlined above underpin the processes and structural styles that develop in all shortening scenarios involving isolated diapirs.

3. Shortening Style of a Single Isolated Diapir

136 Variations in the map-view, profile, size, and orientation with respect to the shortening direction
137 of diapirs means that each salt diapir will respond differently to shortening (e.g. Vendeville and
138 Nilsen, 1995; Callot et al., 2007; Jackson and Hudec, 2017). Irrespective of diapir morphology,
139 the preferential deformation of the salt relative to the surrounding sedimentary rocks leads to the
140 development of generic features that can help determine, to the first order, if a given diapir has
141 been squeezed. These include: i) a narrow or welded-out diapir stem (secondary weld); ii)
142 evidence of diapir rise after the (salt) source layer surrounding the diapir has been depleted; iii) a
143 thick, isopachous, arched sedimentary roof; and iv) shortening structures, that is, folds and
144 thrusts, adjacent to the diapir (e.g. Vendeville and Nilsen, 1995; Gottschalk et al., 2004; Rowan
145 et al., 2004; Roca et al., 2006; Jackson et al., 2008; Dooley et al., 2009; 2015; Jackson and
146 Hudec, 2017). However, to fully recognise the degree of diapir shortening, it is valuable to note
147 the sequence in which map-view structural styles develop as a generic isolated diapir is
148 shortened. For this we assume that the diapir is initially elliptical in map-view here (i.e. a stock),
149 but the generic features described are typical of most common diapir geometries.

150 The sequence of structures that develop during the shortening of an isolated diapir is strongly
151 conditioned by salt's weakness in combination with strain magnitude. At low strains, far-field
152 hinterland shortening thickens the sediment pile driving pressurised source-layer salt towards the
153 foreland and into the diapir (Dooley et al., 2009; 2015). The mechanical weakness of the salt
154 diapir relative to the stronger surrounding sedimentary rocks means that the diapir flanks begin
155 to converge. As this begins the diapir, in this case a circular stock, narrows and rises, and the
156 roof shortens (Fig. 3a) (Nilsen et al., 1995). This squeezing of the diapir and shortening of the
157 roof occurs well ahead of the advancing thrust-front such that the diapir forms a thrust-front
158 salient (Fig. 3a) (Dooley et al., 2009, 2015). At these low strains, even though the diapir and its

159 roof have deformed to accommodate some shortening strain, shortening of the surrounding
160 sedimentary rocks is instead accommodated solely by lateral compaction (e.g. Koyi et al., 2004;
161 Dooley et al., 2009).

162 At intermediate shortening strains, the diapir continues to preferentially accommodate
163 shortening strain relative to the surrounding sedimentary rocks. The salt is significantly
164 pressurised and rises allowing the diapir to narrow in the shortening direction and lengthen
165 normal to the shortening direction (Fig. 3b) (e.g. Nilsen et al., 1995; Callot et al., 2007; Dooley
166 et al., 2009). The key point here is that to maintain kinematic compatibility, thrusts, folds or a
167 combination of both must nucleate at the diapir before propagating out into the adjacent
168 sedimentary rocks (Fig 3b) (Koyi, 1988; Nilsen et al., 1995; Baldschuhn et al., 2001; Rowan et
169 al., 2001; Gottschalk et al., 2004; Letouzey and Sherkati, 2004; Rowan et al., 2004; Callot et al.,
170 2007; Jackson et al., 2008; Fernandez and Kaus, 2014). In particular, faults commonly nucleate
171 on the hinterland side of the diapir and subsequently propagate into the surrounding sedimentary
172 rocks. For these faults, fault portions nearest the diapir will generally be oriented parallel to the
173 shortening direction before curving to strike perpendicular to the shortening direction further
174 away (Fig. 3b) (e.g. Nilsen et al., 1995; Gottschalk et al., 2004; Jackson et al., 2008; Dooley et
175 al., 2015). The slip-vector on the faults thus also changes from strike-slip to dip-slip along the
176 faults. Sub-vertical fault portions adjacent to the diapir that strike parallel to the shortening
177 direction accommodate strike-slip motion (i.e. act as lateral ramps), obliquely-striking fault
178 portions accommodate transpression (i.e. act as oblique ramps), and fault portions further away
179 from the diapirs accommodate reverse fault motion (i.e. act as frontal thrusts) (Fig. 3b). The
180 portions of the faults that strike parallel and obliquely to the shortening direction bound a fault
181 block termed a primary indenter (Fig. 3b) (Dooley et al., 2009; 2015). At intermediate strains the

indenter is a salient in the deformation front that develops as the block in the immediate hinterland of the diapir moves faster towards the foreland that the adjacent strata. The indenter does this because it is moving into the relatively weak diapir and displacing salt (Fig. 3b) (Dooley et al., 2009; 2015).

At high strains, the thrust belt in the sedimentary rocks on either side of the diapir further into the foreland than the diapir, with thrusts converging towards the diapir (Fig. 3c) (Dooley et al., 2015; Jackson and Hudec, 2017). The mechanically weak diapir is partly enveloped within the thrust belt and now forms a re-entrant in the thrust-front (Fig. 3c) (e.g. Dooley et al., 2015). As shortening continues, a series of escape structures develop in the pop-ups flanking the diapir (Fig. 3c) (Dooley et al., 2015). These structures, termed 'secondary indenters', may converge on, and constrict the diapir along transpressional faults.

4. Influence of Roof Thickness on Structural Styles Developed During Shortening of an Isolated Diapir

The classic sequence of structural styles described above commonly occur as a simple diapir shortens, particularly in settings prone to shorten by thrusting. However, differences in diapir roof thickness may complicate the deformation. When a thin-roofed diapir is squeezed, the weak roof is easily deformed, pierced and dismembered by upward flow of salt, and thus salt extrusions and secondary welds are common (e.g. Rowan and Vendeville, 2006; Dooley et al., 2015). In contrast, when a thick-roofed diapir is squeezed, the strong roof is more resistant to deformation and thus will tend to resist major upward flow of salt and piercement (e.g. Rowan and Vendeville, 2006; Dooley et al., 2009). In this case: i) salt extrusions are rare; ii) it is much

205 more difficult to expel sufficient salt to develop secondary welds; and iii) salt is pumped back
206 down into the source layer (Dooley et al., 2009). We now examine structural styles associated
207 with shortening of thin- and thick-roofed diapirs, respectively.
208
209 ***4.1. Styles Associated with Shortening of a Thin-Roofed Diapir***
210 At low strains, as the diapir flanks begin to converge, the diapir narrows and rises. In the
211 presence of a thin, weak roof, the rising salt stretches and uplifts the roof to accommodate a
212 dynamic bulge (Fig. 4) (Dooley et al., 2015). An upturned collar of roof sediments forms as the
213 roof diverts some rising salt towards the diapir periphery to form a peripheral bulge (Dooley et
214 al., 2015). As strain focuses on the diapir and its deformed roof, roof thrusts may form on the
215 foreland or hinterland side of the diapir (Fig. 4a).
216 At intermediate shortening strains, salt in the diapir is significantly pressurised and the diapir
217 continues to narrow and rise. Once the dynamic bulge and thin roof is arched high enough to
218 surmount the upturned collar, the roof spreads outwards, forming both radial and peripheral
219 graben (Fig. 5) (Davison et al., 2000; Dooley et al., 2015). The salt eventually extrudes through
220 the thin, weakened roof either through the radial and peripheral graben, or across the upturned
221 collar (Figs. 4 and 5). At this time, the thin roof dismembers into a series of rafts that are carried
222 away to the periphery of the sheet before grounding and being engulfed by the flow (Figs. 5 and
223 6) (e.g. Dooley et al., 2015). Extruded salt typically flows down-dip towards the foreland, but
224 may also flow into any local lows such as the footwall of an adjacent thrust, and highs created by
225 folds and thrusts may channel salt along-strike (Fig. 6) (see Dooley et al., 2015 for details).
226 At high strains, once the mechanically weak diapir is enveloped within the thrust belt and
227 forms a re-entrant in the thrust front, secondary indenters converge on and constrict the diapir

228 along transpressional faults (Fig. 3c and 6) (Dooley et al., 2015). As the thin-roof has undergone
229 break-up, salt can easily flow upward and extrude as the diapir narrows (Figs. 4 and 6). This
230 increases the likelihood of opposing diapir flanks touching to form a sub-vertical secondary weld
231 that separates an extruded salt sheet above from a triangular pedestal below (Fig. 4b) (e.g.
232 Nielsen et al., 1995; Koyi, 1998; Fort et al., 2004; Roca et al., 2006; Rowan et al., 2012). If
233 shortening continues after the diapir has pinched shut, the sub-vertical secondary weld stem may
234 be offset by a thrust (Fig. 4c) (Callot et al., 2007; Jackson and Hudec, 2017). Dipping secondary
235 welds may be reactivated as thrusts (e.g. Rowan et al., 1999).
236
237 ***4.2. Styles Associated with Shortening of a Thick-Roofed Diapir***
238 Based on the detailed description of how an isolated diapir with a thick-roof accommodates
239 shortening presented by Dooley et al (2009), an isolated thick-roofed diapir shows three
240 differences to a comparable thin-roofed diapir during shortening. First, although the diapir roof
241 arches in both thick- and thin-roof scenarios, in thick-roof examples, the crestal graben that
242 develop typically strike parallel to the shortening direction, whereas in the thin-roof scenario,
243 radial and peripheral graben develop (Withjack and Scheiner, 1982; Dooley et al., 2009, 2015).
244 Second, in the thick-roofed scenario the roof is too strong and cannot break-up and dismember to
245 form roof rafts (Fig. 7) (*cf.* Dooley et al., 2009, 2015). Third, and perhaps most importantly,
246 where the diapir roof is thick and strong, and thus does not break-up, there is no conduit for
247 pressurized salt to extrude (Fig. 7). Consequently, for the diapir flanks to converge, salt in the
248 diapir is pumped downward as an outward plume that is expelled back into the source layer,
249 providing it is thick enough to accommodate this downward and outward flow (Fig. 7) (Dooley
250 et al., 2009).

5. Shortening of an Array of Isolated Diapirs

Having described shortening styles associated with *single* isolated diapirs, we now broaden the scope of our study to describe shortening styles in *arrays* of isolated diapirs so as to explore the consequences for the evolution of the fold-and-thrust belts. Studies examining shortening styles in diapir arrays and the implications for fold-and-thrust belts are relatively rare, the work of and Brun and Fort (2004), Letouzey and Sherkati (2004), Jahani et al. (2009), Callot et al. (2007, 2012), and Fernandez and Kaus (2014) being notable exceptions. During shortening, individual isolated diapirs within the array will essentially behave like single diapirs described in sections 3 and 4, and following the mechanical principles outlined in section 2. However, numerous important questions remain to elucidate, including: i) how do diapirs interact and link with one another?; ii) how does the initial configuration of diapirs influence structural style?; and iii) how and why do structural styles vary across a diapir array?

5.1. How do diapirs interact across a shortened array?

As previously described, diapirs deform more readily than the surrounding sedimentary rocks under compressional stress. In areas prone to buckling, anticlines typically nucleate at, and propagate away from, each of the diapirs (e.g. Fernandez and Kaus, 2014). Anticlines develop rather than synclines as arched (i.e. anticlinal) diapir roofs are amplified by buckling (Callot et al., 2007, 2012; Jahani et al., 2009; Fernandez and Kaus, 2014; Jackson and Hudec, 2017). In contrast, where faulting predominates, thrust, transpressional and tear faults (frontal ramps, oblique ramps and lateral ramps, respectively) generally nucleate at, and propagate outward from

each of the squeezed diapirs (Fig. 8) (Dooley et al., 2009, 2015; Jackson and Hudec, 2017). As shortening strain increases, the faults or folds lengthen, eventually interacting and linking with those from nearby diapirs (Fig. 8b) (Callot et al. 2012; Jackson and Hudec, 2017). A corollary of this is that closely-spaced diapirs will typically link earlier in the shortening history, that is, at lower strains, than widely-spaced diapirs. Mature shortened diapir arrays thus consist of diapirs, or their equivalent welds, that are linked to one another by folds, thrusts or tear faults in the intervening sedimentary rocks (Fig. 8b-c) (Callot et al., 2012).

Settings where a cluster of precursor diapirs are located adjacent to a broad region of flat-lying salt that has no precursor diapirs are also of note. As these settings shorten, each diapir forms a local primary indenter and salient in the deformation front as described previously (e.g. Fig. 3). However, diapir cluster as a whole will form a *composite* primary indenter and deformation front salient relative to the area detached on the unstructured salt. This is due the presence of the mechanically weak salt in the overburden that facilitates a greater rate of propagation of deformation into the foreland in the diapir array than the area detached on unstructured salt.

Overall, these concepts provide a general framework as to how diapirs interact. However, we now consider how the precursor configuration of diapirs controls the geometry, kinematics and orientations of the resultant fold-and-thrust belt (e.g. Callot et al., 2012).

5.2. How does the precursor diapir configuration influence the structural style of fold-and-thrust belts?

Prior to shortening, an array of isolated diapirs may be configured in a variety of ways, for example they may be: i) aligned perpendicular to the shortening direction; or ii) tangentially- or

obliquely offset with respect to one another both parallel to, and perpendicular to, the shortening direction (Fig. 9). These different configurations control the overall structural styles that develop during shortening (Fig. 10). A common configuration in nature, and thus oft-represented in physical models, involves an array of diapirs that are aligned perpendicular to the shortening direction. In buckling-prone settings if diapir arrays are aligned perpendicular to the shortening direction, anticlines nucleate at the diapirs before propagating away along strike, connecting with folds flanking adjacent diapirs. An anticlinal fold belt develops that is oriented perpendicular to the shortening direction; diapirs are located along the axis of the folds (e.g. Fars Province of the Zagros Mountains in Iran: Letouzey and Sherkati, 2004; Jahani et al., 2009; Callot et al., 2012). Note that an exception occurs when precursor diapirs are closely-spaced in the shortening direction, in this case diapirs may be located in the limbs of folds or in synclines (e.g. Rowan, 2003; Jahani et al., 2009; Callot et al. 2012; Fernandez and Kaus, 2014). A similar process to the development of the anticlinal fold chain occurs in fault-prone settings. In these settings, sub-linear fold and thrust belts develop that strike perpendicular to the shortening direction and which show faults that locally curve in toward the diapirs (Fig. 8) (e.g. Lower Congo Basin, Gabon; Jackson et al., 2008).

Arrays of stocks and walls that are not aligned with one another perpendicular to the shortening direction may have varying degrees of offset with one another both parallel- and perpendicular- to the shortening direction (Fig. 9). In these scenarios, the precise arrangement of the diapirs with respect to one another, along with the roof thickness, will control the type and orientation of structures that develop to connect the diapirs. Where thin-roofed diapirs are tangentially offset from one another, faults nucleate at, and propagate away along-strike from, each of the diapirs (Fig. 10a). The striking feature in this particular configuration is that the

319 diapirs link to one another via a single tear fault, or series of small tear faults within a narrow
320 strike-slip fault zone, oriented parallel to the shortening direction. In contrast, if the diapir roof is
321 thick, the diapirs may link by the formation of a pop-up structure that is oriented oblique to the
322 shortening direction. Where thin-roofed diapirs are obliquely-offset from one another, the diapirs
323 link to one another via a transpressional pop-up structure oriented oblique to the shortening
324 direction (Fig. 10b). On the other hand, if the roof is thick, faults that propagate away from the
325 diapirs may curve at their tips to link the obliquely-offset diapirs.

326 A further consideration is the degree of connectivity of the diapirs prior to shortening. In
327 some cases, such as in the sub-canopy system of the northern Gulf of Mexico, the isolated diapirs
328 are connected at depth by a polygonal network of buried salt anticlines or ridges (Fig. 11). These
329 anticlines or ridges radiate and plunge away from each of the diapirs to form an egg-carton-like
330 precursor geometry (Fig. 11) (Rowan and Vendeville, 2006). During shortening, both the diapirs
331 *and* the deep anticlines or ridges localize the shortening strain. As such, faults and folds nucleate
332 at the diapirs, and propagate away following the axes of the deep anticlines or ridges. The result
333 is a polygonal network of faults and folds in the supra-salt that reflects the map-view pattern of
334 the underlying anticlines or ridges (e.g. Rowan and Vendeville, 2006). It is likely that the more
335 deeply-buried the anticlines or ridges are relative to the isolated diapirs, the lesser the effect they
336 will have upon the final map-view pattern of faults or folds. This type of system, and the map-
337 view geometries developed, differ markedly to the sub-linear fold-and thrust belts developed
338 during shortening of provinces with completely unconnected precursor isolated diapirs.

339

340 ***5.3. How and why do structural styles vary across a diapir array?***

There are two fundamental reasons as to why structural styles vary across a diapir array. First, shortening strains must propagate across the array in the dip direction, so some diapirs within the array may be more strained than others. In systems driven by plate tectonics (e.g. Fars Province of the Zagros Mountains in Iran, Betic foreland, Pyrenean foreland), shortening strains propagate from the hinterland toward the foreland, thus diapirs located closer to the hinterland will be shortened earlier and to a higher degree than those located towards the foreland. In contrast, in gravity-driven slope systems, strain propagation is much more variable. Important factors include the presence or absence of a buttress, critical taper geometry, salt thickness, the location of the salt pinchout, the presence of hinges in the detachment surface, the location of the base of slope, overburden strength, and strain rate (e.g. Letouzey et al., 1995; Dooley et al., 2007, 2013; Jackson et al., 2008; Morley et al., 2011).

The second reason is that diapirs within an array may show variations in cross-sectional profile, map-view geometry, size, and orientation of diapirs with respect to the shortening direction. Furthermore, there may also be spatial variations in the style and degree in which pre-existing faults influence the sedimentary rocks surrounding the diapirs. These types of variations result in the development of different structural styles during shortening (Roca et al., 2006; Callot et al., 2007; Jackson and Hudec, 2017). A complete discussion of these variables is beyond the scope of this study, however, we comment on two of the most important factors.

First, diapirs with different cross-sectional profiles respond to shortening in varying ways. For example, initially narrow diapirs rise higher and faster than wide diapirs during shortening. Higher and faster rising salt results in more steeply-arched roofs above initially narrow diapirs (Fig. 12a) (Nilsen et al., 1995). Variations in the angle of the salt-sediment interface at the diapir flanks may also influence structural style development. Low-angle salt-

sediment interfaces can act as thrust ramps (Fig. 12b) (Callot et al., 2007). In contrast, steep salt-sediment interfaces are not favourably oriented for thrusting. Short-cut thrusts may thus form at or near the base of the diapir, passively transporting a large part of the diapir in the developing fold in the thrust hanging-wall (Fig. 12b) (see Callot et al., 2007 for further details).

Second, there may be a range of map-view diapir geometries within the precursor diapir array, in particular salt walls may have different orientations with respect to the shortening direction (Figs. 12c and d). For example, some walls may have their long axis oriented perpendicular to the shortening direction (perpendicular walls) whereas other walls may have their long axis parallel or oblique to the shortening direction (parallel walls and oblique walls, respectively). Each of these will respond differently to shortening (Figs. 12c-d and 13). Perpendicular walls are the easiest to weld shut because they maximize the volume of expelled salt for an increment of shortening (Fig. 12d). However, the strength of sedimentary rocks around the ends of the wall means that the centre of the wall may be squeezed more than the ends. The tips may thus resist welding leaving two remnant diapirs connected by a vertical weld (e.g. La Popa weld in Rowan and Vendeville, 2006) (Fig. 12c). Parallel walls extrude much less than perpendicular walls given the same amount of shortening and require therefore more shortening to close (Fig. 12d). Structural styles become more complex with oblique walls and can vary according to the degree obliquity to the shortening direction (Fig. 13). Oblique walls experience transpressional stresses and hence form uplifts bounded by oblique-slip reverse faults. Furthermore, the ends of oblique walls, and any faults emanating from their tips, curve progressively to align with regionally-oriented thrust faults; thus oblique walls commonly display sigmoidal map-view geometries (e.g. Gottschalk et al., 2004; Callot et al., 2012) (Fig. 13).

6. Conceptual Models of Shortening in Isolated-Diapir Provinces

Based on the preceding observations from natural and physically-modelled systems, we present a series of conceptual models that synthesise how roof thickness, diapir configuration, and shortening magnitude influence structural styles developed during shortening of isolated-diapir arrays (Figs. 14 and 15). The pre-shortening configuration of the models is shown in Figure 2. The models assume that shortening is thin-skinned and propagates from the hinterland on the right, to the foreland on the left. Comparing structural styles in the foreland and hinterland we thus capture temporal evolution at increasing strain. We also assume no syn-shortening sedimentation, erosion, or variation in shortening rates. We vary roof thickness and strain magnitude.

6.1. Thin-Roofed Scenarios

At low strains (Fig. 14a), diapir roofs in the foreland are captured early in the process of break-up, with arching and crestal faulting being dominant. In contrast, diapirs roofs located towards the hinterland are more highly-strained, with overturned flaps, extrusive salt sheets and roof rafts being common. In a similar vein, less-strained diapirs toward the foreland remain open in section view as salt continues to flow into the diapir, whereas the flanks of more highly-strained diapirs toward the hinterland are welded shut at the waist. The connectivity of tear faults, transpressional, and thrust faults emanating from the diapirs is low. The diapir array is not connected by faults and swathes of the sedimentary rocks between the diapirs are largely undeformed.

409 At high strains, all diapirs in the array, even those located toward the foreland, experience
410 strong deformation (Fig. 14b). Diapirs tend to be welded shut, with some secondary welds
411 reactivated as thrusts, or, in the case of very high strains, offset by short-cut thrusts. The
412 convergence of diapir flanks that is required to weld the diapirs is facilitated by break-up of the
413 weak diapir roofs and subsequent extrusion of salt sheets. If the diapirs are relatively closely-
414 spaced, the salt sheets may coalesce to form a canopy.

415 There are several key differences between the high- and low-strain scenarios (*cf.* Figs.
416 14a and b). First, at high strains, the diapirs form local re-entrants in the deformation front rather
417 than the salients observed at low strains. Second, at high strains, the faults and folds emanating
418 from each diapir have lengthened and linked with those from adjacent diapirs. Thrust faults and
419 folds link diapirs that are broadly along-strike (or obliquely-offset) from each other, whereas tear
420 faults link diapirs that are tangentially offset from one another parallel to the shortening
421 direction. Third, at high strains, once the diapirs are welded shut, they eventually lock up and
422 deformation migrates to any remaining open diapirs further toward the foreland.

423

424 ***6.2. Thick-Roofed Scenarios***

425 At relatively low strains, thick-roofed settings show some similarities in structural style to
426 mildly-strained thin-roofed settings (*cf.* Figs 14a and 15a). Diapir roofs toward the foreland are
427 only gently arched, whereas diapir roofs towards the hinterland display more faulting and
428 folding. Second, faults and folds remain unlinked and the diapir network is poorly connected.
429 The major differences between thick-roofed and thin-roofed diapir arrays at low strains are that
430 thick-roofed diapirs are much more likely to remain open in cross-section and much less likely to

extrude salt. These differences are a result of the thick and strong diapir roofs that do not easily deform to facilitate diapir flank convergence or break-up to permit salt extrusion.

In highly-strained settings, diapirs are to some extent connected to other diapirs by faults, although the degree of connectivity is not as high as in the thin-roofed scenario (*cf*. Figs 14b and 15b). There are also some key differences. Most importantly, the roofs are too strong to break-up and provide conduits for salt extrusion, so little or no salt is observed at surface. The inability of salt to extrude in thick-roofed settings means that diapirs are more difficult to weld, since there is no easy exit for displaced salt. Some displaced salt forms remnant bulbs at shallow levels and more may be pumped downwards as outward plumes into the source layer. These outward plumes thicken the source layer and hydraulically lift fault blocks, perhaps facilitated by a distal thrust at the edge of salt (Dooley et al., 2009). Pumping salt down into the source layer and lifting up sediments requires much more force than simply having salt rise and extrude at the surface as occurs in thin-roofed scenarios, and requires much higher salt pressures. Thus, not all the salt may be expelled from the diapirs, and some diapirs may just be narrowed rather than welded.

7. The Influence of Precursor Isolated Diapirs on the Styles of Fold-and-Thrust Belts

If sedimentary basins do not contain diapirs prior to thin-skinned shortening, the map-view configurations of the fold-and-thrust belts that develop are relatively simple (Fig. 16). Fold and thrust traces are sub-linear to curvilinear in form, are regularly-spaced across-strike, and are

453 commonly continuous over lengths of 100 km or more with little variation in structural style.
454 Deformation fronts are broadly linear and continuous along-strike.
455 In contrast, when sedimentary basins containing precursor isolated diapirs are shortened the fold-
456 and-thrust belts become much more complex (Figs. 14 and 15). Many of these key styles are
457 expressed in the Fars Region of the Zagros Mountains in Iran, an area that contained isolated
458 diapirs prior to Neogene shortening (Fig. 17a) (Letouzey and Sherkati, 2004; Callot et al. 2007;
459 2012; Jahani et al., 2009). Although structures define a fold-and-thrust belt aligned broadly
460 perpendicular to the shortening direction as in the non-diapiric settings in Figure 16, there are
461 also three key differences to those settings. First, fold axes are much shorter (20-80 km) than
462 those seen for example in the Canadian Rockies and the Appalachians (>>100 km) (e.g. Bally et
463 al., 1966; Frey, 1973; Davis and Engelder, 1985). Second, a large number of salt extrusions are
464 present, marking the locations of the pre-existing diapirs (Callot et al., 2007). Third, the diapirs
465 are connected to one another by the network of fold and thrusts, resulting in local deviations in
466 the trends of these structures in the fold-and-thrust belt (Fig. 17a). This configuration is also
467 expressed, albeit at a smaller scale, in the Astrid Fold Belt, Lower Congo Basin, offshore Gabon
468 (Jackson et al., 2008) (Fig. 17b). Overall, this process of fold and fault nucleation at squeezed
469 diapirs and subsequent propagation and linkage of these structures to form a connected fault/fold
470 network is fundamental to the evolution of shortened isolated-diapir provinces (Figs. 8, 10, 14,
471 15).

472 As shown here, salt provinces may differ in structural style due to variations in degree of
473 shortening and in pre-shortening salt configuration. An entirely different style of salt-involved
474 shortening occurs where pre-shortening minibasins lie adrift in a sea of salt, that is, they are
475 surrounded by salt walls on all sides (*isolated-minibasin provinces*). If the relatively modest

amounts of salt present in isolated-diapirs cause such major changes in structural style, what happens when there is an order of magnitude more salt (e.g. Duffy et al., 2017)? An analysis of these systems will form the basis of a future study.

8. Conclusions

- Shortening styles in salt basins containing diapirs depend largely upon the pre-shortening configuration of the diapirs. We recognize two end-member pre-shortening diapir configurations. In the first, isolated diapirs are encased in a relatively rigid sediment body (*isolated-diapir provinces*). In the second, isolated minibasins are surrounded by salt walls and the minibasins are effectively adrift within a 'sea of salt' (*isolated-minibasin provinces*).

- This study examined structural styles associated thin-skinned shortening of isolated-diapir provinces. We found that even though isolated-diapirs form volumetrically minor components of sedimentary basins, they have a disproportionately large influence on structural style due to the relative weakness of rock salt and its ability to localize strain.

- The structural styles developed during shortening of isolated-diapir provinces are governed to a large extent by three mechanical principles. First, diapirs shorten prior to surrounding sedimentary rocks due to their relative weakness. Second, diapirs nucleate folds and faults that propagate out into the surrounding sedimentary rocks. Third, as

diapirs are squeezed, the roof must also shorten; extrusive salt sheets are expelled through thin roofs, whereas thicker roofs resist piercement but may still be faulted and folded.

- In shortened isolated-diapir arrays, faults and folds nucleate at, and propagate away from individual diapirs. These folds and faults link up with structures from adjacent diapirs so that diapirs are all connected. However, the precise configuration of the diapirs with respect to one another, along with roof thickness, will control the style and orientation of structures that connect the diapirs.

- First-order controls on the structural styles in shortened isolated-diapir provinces are pre-shortening configuration and degree of connectivity of diapirs, strain magnitude and diapir roof thickness. Second order controls on structural style development include: initial diapir cross-sectional profiles, map-view geometry of diapirs, diapir size, and diapir orientation with respect to the shortening direction.

- Structural styles of fold-and-thrust belts developed in basins with isolated-diapirs developed prior to shortening (e.g. Fars Region of the Zagros Mountains and the Astrid Fold Belt in the Lower Congo Basin of Offshore Gabon) exhibit more complex geometries and greater spatial variability in structural styles than fold-and-thrust belts developed above a simple décollement (e.g. Southern Canadian Rockies and the Appalachian Plateau, USA).

9. Acknowledgements

We would like to thank Nancy Cottington for figure drafting, particularly the 3D conceptual models and Frank Peel, Gillian Apps, and Maggie Curry for discussions that helped refine this work. The project was funded by the Applied Geodynamics Laboratory (AGL) Industrial Associates program, comprising the following companies: Anadarko, Aramco Services, BHP Billiton, BP, CGG, Chevron, Condor, EcoPetrol, EMGS, ENI, ExxonMobil, Hess, Ion-GXT, Midland Valley, Murphy, Nexen USA, Noble, Petrobras, Petronas, PGS, Repsol, Rockfield, Shell, Spectrum, Statoil, Stone Energy, TGS, Total, WesternGeco, and Woodside (http://www.beg.utexas.edu/agl/sponsors). The authors received additional support from the Jackson School of Geosciences, The University of Texas at Austin. The stay of Juan I. Soto at the Bureau of Economic Geology has been funded by a Salvador de Madariaga fellowship of the Ministerio de Educación, Cultura y Deporte, Spain.

10. Figure Captions

Fig. 1. Style of shortening depends on the relative thicknesses of overburden and salt along with whether or not diapirs were present prior to the onset of shortening. These forward models maintain salt area through time (after Hudec and Jackson 2007).

Fig. 2. Schematic figure showing a pre-shortening configuration typical of an 'isolated-diapir province' with discrete salt stocks and walls. Sequences coloured in blue represent sediment deposited during the growth of the diapirs and prior to the deposition of the roof (green units). Dark green unit, if imagined that it covers across the entire area of model, represents what we term a thin roof. Light green unit, if imagined that it covers across the entire area of model, represents what we term a thick roof.

Fig. 3. Schematic structural evolution of a shortened isolated diapir (in this case, a stock) in map view. a) initial squeezing and associated salt rise in the diapir in advance of the deformation front; b) fault-bounded primary indenter block moves into a yielding diapir; the diapir forms a salient in the deformation front; c) diapir changes from a salient in the deformation front to a re-entrant; secondary indenters converge on and constrict the diapir. Based on physical models in Dooley et al. (2015).

Fig. 4. Series of cross-sections through a thin-roofed isolated diapir at increasing degrees of shortening. Cross-sections are oriented parallel to the shortening direction. a) at low strain the squeezed diapir remains open but the roof is arched; b) at intermediate strain the diapir is squeezed shut to form a vertical secondary weld and the salt has extruded through the thin roof leaving an overturned flap; and c) at high

strains the vertical secondary weld has been offset by a new shortcut thrust (note that in some cases, the secondary weld can be reactivated as a thrust weld, particularly if the initial weld was dipping).

Fig. 5. Roof break-up sequence of an isolated thin-roofed diapir (stock) at increasing degrees of shortening strain (after Dooley et al., 2015). a) radial and peripheral grabens form in the uplifting stretched roof; b) as shortening increases, the pressurised salt continues to rise, breaking through the weak radial and peripheral grabens in the roof; c) salt lobes extrude through the weak points in the roof before coalescing. R1 to R5 refer to individual portions of the roof or rafts.

Fig. 6. Overhead views of a physical model of a single isolated diapir (a stock) with a thin roof at various degrees of shortening strain. a) at very low strain the roof above the squeezed diapir is uplifted and radial and peripheral graben form; diapir forms a salient in the deformation front; b) as strain increases the diapir roof breaks up and the salt extrudes; c) at intermediate shortening strains salt continues to extrude, flowing towards the foreland (left); faults nucleate on the hinterland side (right) of the squeezed stock and propagate outwards to define a primary indenter block that drives into the diapir; d) at high shortening strains there is massive salt extrusion, secondary indenters and pop-ups developed adjacent to the diapir, which forms a re-entrant in the deformation front.

Fig. 7. Overhead and cross-section views showing key structural styles associated with shortening of single isolated diapir with a thick roof (modified from Dooley et al., 2009). Shortening direction in all models is from the right to left. a) Overhead view at mild shortening strains (7.5 cm) and b) cross-section through a) along line of section x-x'. Note how the inward plume of salt inflates the diapir. c) Overhead view at intermediate shortening strains (15 cm) and d) cross-section through c) along line of section y-y'. e) Overhead view at high shortening strains (30 cm) and f) cross-section through e) along line of section z-z'. Note how salt is not extruded at the surface and how salt is pumped out of the diapir and into the source layer via a major outward plume. e) is at the same scale as a) and c) but the field of view has shifted to show the basin-edge thrust.

Fig. 8. Overhead views of a physical model of an array of diapirs (stocks) that are aligned perpendicular to the shortening direction (each diapir had a thick roof). Blue circles show the initial location of the diapirs. At low shortening strains (a) minimal deformation is observed. At moderate shortening strains (b) diapirs preferentially localise shortening strain so faults and folds nucleate at diapirs and propagate out into the surrounding sedimentary rocks. At strong degrees of shortening (c) the faults and folds have propagated laterally such that they now link the diapirs perpendicular to the shortening direction.

Fig. 9. Sketch showing in map-views of different diapir (stock) configurations: a) diapirs aligned perpendicular to the shortening direction; b) tangentially-offset diapirs (tangent parallel to shortening direction) and c) obliquely-offset diapirs. Diapirs are pink. White arrow shows the shortening direction.

Fig. 10. Overhead views showing the result of shortening two thin-roofed isolated diapirs (stocks). The configuration of the diapirs prior to shortening determines the style in which diapirs connect during shortening. a) tangentially-offset salt stocks are connected by tear faults. b) obliquely-offset diapirs are connected by a transpressional pop-up structure.

Fig. 11. Map showing portion of the present-day sub-canopy system of the northern Gulf of Mexico where isolated diapirs (diapir roots shown in red; grey if inferred) are connected at depth by buried anticlines or ridges of salt (pink). Black dashed lines are outlines of where shallow salt extruded from the diapir roots. Map of Miocene structural elements are overlain: green lines show normal faults that record extension and/or salt withdrawal; red lines indicate areas of shortening (e.g. folds, thrusts, and squeezed diapirs); and blue lines indicate areas with a likely predominance of strike-slip deformation. The black arrows indicate the shortening direction. After Rowan and Vendeville (2006).

Fig. 12. Schematic diagrams showing the influence of the initial cross-sectional profile (a and b) and the map-view geometry (c and d) of the precursor diapir on the structural style developed during shortening. a) initially narrow diapirs rise more than wide diapirs (from Nilsen et al., 1995); b) influence of cover thickness and angle of the salt-sediment interface on the diapir flanks upon structural style developed during shortening (Callot et al., 2007); c) conceptual model of a salt wall that is oriented perpendicular to the shortening direction. The strength of rocks around the wall tips mean it is harder to squeeze the tips of the wall than the ends. When the wall preferentially welds in the centre, leaving two remnant diapirs at the ends ('Q-tips') that are connected by a secondary weld (Rowan and Vendeville, 2006); d) differences in how a perpendicular wall (wall with long axis oriented perpendicular to the shortening direction) and parallel wall (wall with long axis oriented parallel to the shortening direction) respond to incremental shortening (stage 1 is the lowest strain and stage 3 is the highest strain). A-A' and B-B' are schematic cross-sections through the perpendicular wall before and after shortening, respectively. C-C' and D-D' show schematic cross-sections through the parallel wall before and after shortening, respectively. Walls in d) are all assumed to have the same area and volume prior to the shortening.

Fig. 13. Overhead views (a and b) and oblique view (c) of a physical model that involved a series of elongate, thin-roofed salt walls with the long axes oriented parallel to, perpendicular to, and at various degrees of obliquity to the shortening direction. Walls A, B, C are broadly aligned with one another as are walls 1, 2, 3 and 4. a) elevation map of the top model surface at mild shortening showing walls oriented oblique to the shortening direction (2, 3, A to C) are squeezed in the foreland (left) of the regional deformation front; obliquely-oriented walls experience transpression and crestal faults developed in the roofs of walls develop in transtension (walls B and C). b) view at intermediate shortening showing extrusion of salt from the walls; c) elevation map showing how the ends of the oblique walls B and C have curved to strike perpendicular to the shortening direction such that the walls display sigmoidal geometries in map-view.

Fig. 14. 3D conceptual block models showing the evolution of structural styles at a) at low strain, and b) at high strain during the shortening of a province of isolated *thin-roofed* diapirs. Same colour legend as in Fig. 2.

Fig. 15. 3D conceptual block models showing the evolution of structural styles at a) at low strain, and b) at high strain during the shortening of a province of isolated *thick-roofed* diapirs. Same colour legend as in Fig. 2.

Fig. 16. Map-view of key structural elements of fold-and-thrust belts that developed without diapirs present prior to shortening: a) a fold-and-thrust belt developed in the absence of a salt decollement in the Southern Canadian Rockies (Bally et al., 1966); and b) a fold-and-thrust belt developed above a salt decollement in the Appalachian Plateau, USA (after Frey, 1973; Chen, 1977; Mesolella, 1978; Davis and Engelder, 1985). Both a) and b) shown at same scale. Note how fault traces and fold axes extend continuously for over 100 km without a significant change in strike and vergence.

Fig. 17. a) Map-view of key structural elements of the Fars Province of the Zagros fold-and-thrust belt in the mountains of Iran; isolated-diapirs were present prior to the onset of shortening (modified from Callot et al. 2012 that was compiled from a geological map of the National Iranian Oil Company). Fold axes are not as long as the fault traces in Fig 16, folds largely appearing to connect salt extrusions. b) Map-view taken from Jackson et al. (2008) from the Astrid Fold Belt in the Lower Congo Basin (offshore Gabon) showing a series of allochthonous sheets (proxies for the locations of isolated diapirs) connected by thrust faults and tear faults. Thrust faults typically strike perpendicular to the shortening direction.

11. References

Bally, A.W., Gordy, P., Stewart, G.A., 1966. Structure, seismic data, and orogenic evolution of southern Canadian Rocky Mountains. Bulletin of Canadian Petroleum Geology 14, 337-381.

Bega, Z., Soto, J., 2017. The Ionian Fold-and-Thrust Belt in Central and Southern Albania: A Petroleum Province With Triassic Evaporites, *in* Permo-Triassic Salt Provinces of Europe, North Africa and the Atlantic Margins. Elsevier, pp. 517-539.

Boyer, S.E., Elliott, D., 1982. Thrust systems. AAPG Bulletin 66, 1196-1230.

Brun, J.-P., Fort, X., 2004. Compressional salt tectonics (Angolan margin). Tectonophysics 382, 129-150.

Callot, J.P., Jahani, S., Letouzey, J., 2007. The role of pre-existing diapirs in fold and thrust belt development, Thrust Belts and Foreland Basins. Springer, pp. 309-325.

Callot, J.-P., Trocmé, V., Letouzey, J., Albouy, E., Jahani, S., Sherkati, S., 2012. Pre-existing salt structures and the folding of the Zagros Mountains. Geological Society, London, Special Publications 363, 545-561.

Cámara, P., Flinch, J.F., 2017. The Southern Pyrenees: A Salt-Based Fold-and-Thrust Belt, *in* Permo-Triassic Salt Provinces of Europe, North Africa and the Atlantic Margins. Elsevier, pp. 395-415.

Canérot, J., Hudec, M.R., Rockenbauch, K., 2005. Mesozoic diapirism in the Pyrenean orogen: Salt tectonics on a transform plate boundary. AAPG Bulletin 89, 211-229.

Carola, E., Muñoz, J.A., Roca, E., 2015. The transition from thick-skinned to thin-skinned tectonics in the Basque-Cantabrian Pyrenees: The Burgalesa Platform and surroundings. International Journal of Earth Sciences 104, 2215-2239.

Chen, P., 1977. Lower Paleozoic Stratigraphy, Tectonics, Paleogeography, and Oil/gas Possibilities in the Central Appalachians (West Virginia and Adjacent States):(also: Oil and Gas Potential of the Lower Paleozoic of West Virginia).

Dahlstrom, C., 1969. Balanced cross sections. Canadian Journal of Earth Sciences 6, 743-757.

Davis, D.M., Engelder, T., 1985. The role of salt in fold-and-thrust belts. Tectonophysics 119, 67-88.

Davison, I., Alsop, G., Evans, N., Safaricz, M., 2000. Overburden deformation patterns and mechanisms of salt diapir penetration in the Central Graben, North Sea. Marine and Petroleum Geology 17, 601-618.

Dooley, T., Jackson, M., Hudec, M., 2015. Breakout of squeezed stocks: dispersal of roof fragments, source of extrusive salt and interaction with regional thrust faults. Basin Research 27, 3-25.

Dooley, T.P., Jackson, M., Hudec, M.R., 2007. Initiation and growth of salt-based thrust belts on passive margins: results from physical models. Basin Research 19, 165-177.

Dooley, T.P., Jackson, M.P., Hudec, M.R., 2009. Inflation and deflation of deeply buried salt stocks during lateral shortening. Journal of Structural Geology 31, 582-600.

687 Duffy, O.B., Fernandez, N., Hudec, M.R., Jackson, M.P., Burg, G., Dooley, T.P., Jackson, C.A.-L., 2017. Lateral mobility of
688 minibasins during shortening: Insights from the SE Precaspian Basin, Kazakhstan. Journal of Structural Geology. 97,
689 257-276.
690
691 Fernandez, N., Kaus, B.J., 2014. Influence of pre-existing salt diapirs on 3D folding patterns. Tectonophysics 637, 354-
692 369.
693
694 Flinch, J., Soto, J., 2017. Allochthonous Triassic and Salt Tectonic Processes in the Betic-Rif Orogenic Arc, *in* Permo-
695 Triassic Salt Provinces of Europe, North Africa and the Atlantic Margins. Elsevier, pp. 417-446.
696
697 Fort, X., Brun, J.-P., Chauvel, F., 2004. Salt tectonics on the Angolan margin, synsedimentary deformation processes.
698 AAPG Bulletin 88, 1523-1544.
699
700 Frey, M.G., 1973. Influence of Salina salt on structure in New York-Pennsylvania part of Appalachian Plateau. AAPG
701 Bulletin 57, 1027-1037.
702
703 Georgiev, G., Tari, G., 2017. Salt Tectonics in the Carnian Evaporite Basin of the Eastern Balkan-Forebalkan Region of
704 Bulgaria, *in* Permo-Triassic Salt Provinces of Europe, North Africa and the Atlantic Margins. Elsevier, pp. 483-497.
705
706 Gottschalk, R.R., Anderson, A.V., Walker, J.D., Da Silva, J.C., 2004. Modes of contractional salt tectonics in Angola Block
707 33, Lower Congo basin, west Africa, Salt-sediment interactions and hydrocarbon prospectivity: 24th Annual Research
708 Conference, Gulf Coast Section, SEPM Foundation. SEPM, pp. 705-734.
709
710 Grelaud, S., Sassi, W., de Lamotte, D.F., Jaswal, T., Roure, F., 2002. Kinematics of eastern Salt Range and South Potwar
711 basin (Pakistan): a new scenario. Marine and Petroleum Geology 19, 1127-1139.
712
713 Guellec, S., Lajat, D., Mascle, A., Roure, F., Tardy, M., 1990. Deep seismic profiling and petroleum potential in the
714 western Alps: Constraints with ECORS data, balanced cross-sections and hydrocarbon modeling. The Potential of
715 Deep Seismic Profiling for Hydrocarbon Exploration. Edition Technip, Paris, 425-437.
716
717 Harrison, J., Jackson, M., 2014. Exposed evaporite diapirs and minibasins above a canopy in central Sverdrup Basin,
718 Axel Heiberg Island, Arctic Canada. Basin Research 26, 567-596.
719
720 Hudec, M.R., Jackson, M.P., Vendeville, B.C., Schultz-Ela, D.D., Dooley, T.P., 2011. The salt mine: A digital atlas of salt
721 tectonics. Bureau of Economic Geology.
722
723 Jackson, M.P., Hudec, M.R., 2017. Salt tectonics: Principles and practice. Cambridge University Press.
724
725 Jackson, M.P., Hudec, M.R., Jennette, D.C., Kilby, R.E., 2008. Evolution of the Cretaceous Astrid thrust belt in the
726 ultradeep-water Lower Congo Basin, Gabon. AAPG Bulletin 92, 487-511.
727
728 Jahani, S., Callot, J.P., Letouzey, J., Frizon de Lamotte, D., 2009. The eastern termination of the Zagros Fold-and-Thrust
729 Belt, Iran: Structures, evolution, and relationships between salt plugs, folding, and faulting. Tectonics 28.6.
730
731 Kergaravat, C., Ribes, C., Callot, J.-P., Ringenbach, J.-C., 2017. Tectono-stratigraphic evolution of salt-controlled
732 minibasins in a fold and thrust belt, the Oligo-Miocene central Sivas Basin. Journal of Structural Geology 102, 75-97.
733
734 Kergaravat, C., Ribes, C., Legeay, E., Callot, J.P., Kavak, K.S., Ringenbach, J.C., 2016. Minibasins and salt canopy in
735 foreland fold-and-thrust belts: The central Sivas Basin, Turkey. Tectonics 35.6, 1342-1366.
736
737 Koyi, H., 1988. Experimental modeling of role of gravity and lateral shortening in Zagros mountain belt. AAPG Bulletin
738 72, 1381-1394.
739

740 Koyi, H.A., Sans, M., Teixell, A., Cotton, J., Zeyen, H., 2004. The significance of penetrative strain in the restoration of
741 shortened layers—Insights from sand models and the Spanish Pyrenees, *in* Thrust tectonics and hydrocarbon systems.
742 AAPG Memoir 82, 207-222
743
744 Leitner, C., Spötl, C., 2017. The eastern Alps: Multistage development of extremely deformed evaporites, *in* Permo-
745 Triassic Salt Provinces of Europe, North Africa and the Atlantic Margins. Elsevier, pp. 467-482.
746
747 Letouzey, J., Colletta, B., Vially, R., Chermette, J., 1995. Evolution of salt-related structures in compressional settings, in
748 Salt tectonics: a global perspective. AAPG Memoir 65, 41-60.
749
750 Lickorish, W.H., Ford, M., 1998. Sequential restoration of the external Alpine Digne thrust system, SE France,
751 constrained by kinematic data and synorogenic sediments. Geological Society, London, Special Publications 134, 189-
752 211.
753
754 Mesolella, K.J., 1978. Paleogeography of some Silurian and Devonian reef trends, central Appalachian Basin. AAPG
755 Bulletin 62, 1607-1644.
756
757 Morley, C., King, R., Hillis, R., Tingay, M., Backe, G., 2011. Deepwater fold and thrust belt classification, tectonics,
758 structure and hydrocarbon prospectivity: A review. Earth-Science Reviews 104, 41-91.
759
760 Nilsen, K.T., Vendeville, B.C., Johansen, J.-T., 1995. Influence of regional tectonics on halokinesis in the Nordkapp Basin,
761 Barents Sea, in Salt tectonics: a global perspective. AAPG Memoir 65, 413-436.
762
763 Roca, E., Muñoz, J.A., Ferrer, O., Ellouz, N., 2011. The role of the Bay of Biscay Mesozoic extensional structure in the
764 configuration of the Pyrenean orogen: Constraints from the MARCONI deep seismic reflection survey. Tectonics 30.2.
765
766 Roca, E., Sans, M., Koyi, H.A., 2006. Polyphase deformation of diapiric areas in models and in the eastern Prebetics
767 (Spain). AAPG Bulletin 90, 115-136.
768
769 Rowan, M.G., Jackson, M.P., Trudgill, B.D., 1999. Salt-related fault families and fault welds in the northern Gulf of
770 Mexico. AAPG Bulletin 83, 1454-1484.
771
772 Rowan, M.G., Lawton, T.F., Giles, K.A., 2012. Anatomy of an exposed vertical salt weld and flanking strata, La Popa
773 Basin, Mexico. Geological Society, London, Special Publications 363, 33-57.
774
775 Rowan, M.G., Lawton, T.F., Giles, K.A., Ratliff, R.A., 2003. Near-salt deformation in La Popa basin, Mexico, and the
776 northern Gulf of Mexico: A general model for passive diapirism. AAPG Bulletin 87, 733-756.
777
778 Rowan, M.G., Peel, F.J., Vendeville, B.C., 2004. Gravity-driven fold belts on passive margins, in Thrust tectonics and
779 hydrocarbon systems. AAPG Memoir 82, 157-182.
780
781 Rowan, M.G., Vendeville, B.C., 2006. Foldbelts with early salt withdrawal and diapirism: physical model and examples
782 from the northern Gulf of Mexico and the Flinders Ranges, Australia. Marine and Petroleum Geology 23, 871-891.
783
784 Sherkati, S., Letouzey, J., Frizon de Lamotte, D., 2006. Central Zagros fold-thrust belt (Iran): New insights from seismic
785 data, field observation, and sandbox modeling. Tectonics 25. 4.
786
787 Sommaruga, A., Mosar, J., Schori, M., Gruber, M., 2017. The role of the Triassic evaporites underneath the North Alpine
788 Foreland, *in* Permo-Triassic Salt Provinces of Europe, North Africa and the Atlantic Margins. Elsevier, pp. 447-466.
789
790 Trudgill, B.D., Rowan, M.G., Fiduk, J.C., Weimer, P., Gale, P.E., Korn, B.E., Phair, R.L., Gafford, W.T., Roberts, G.R., Dobbs,
791 S.W., 1999. The perdido fold belt, northwestern deep gulf of mexico, part 1: Structural geometry, evolution and
792 regional implications. AAPG Bulletin 83, 88-113.
793

794 Velaj, T., Davison, I., Serjani, A., Alsop, I., 1999. Thrust tectonics and the role of evaporites in the Ionian Zone of the
795 Albanides. AAPG Bulletin 83, 1408-1425.
796
797 Vendeville, B.C., Nilsen, K.T., 1995. Episodic growth of salt diapirs driven by horizontal shortening, Salt, Sediment, and
798 Hydrocarbons. SEPM Gulf Coast Section 16th Annual Research Foundation Conference, pp. 285-295.
799
800 Withjack, M.O., Scheiner, C., 1982. Fault patterns associated with domes--an experimental and analytical study. AAPG
801 Bulletin 66, 302-316.
802

803

804

805

806

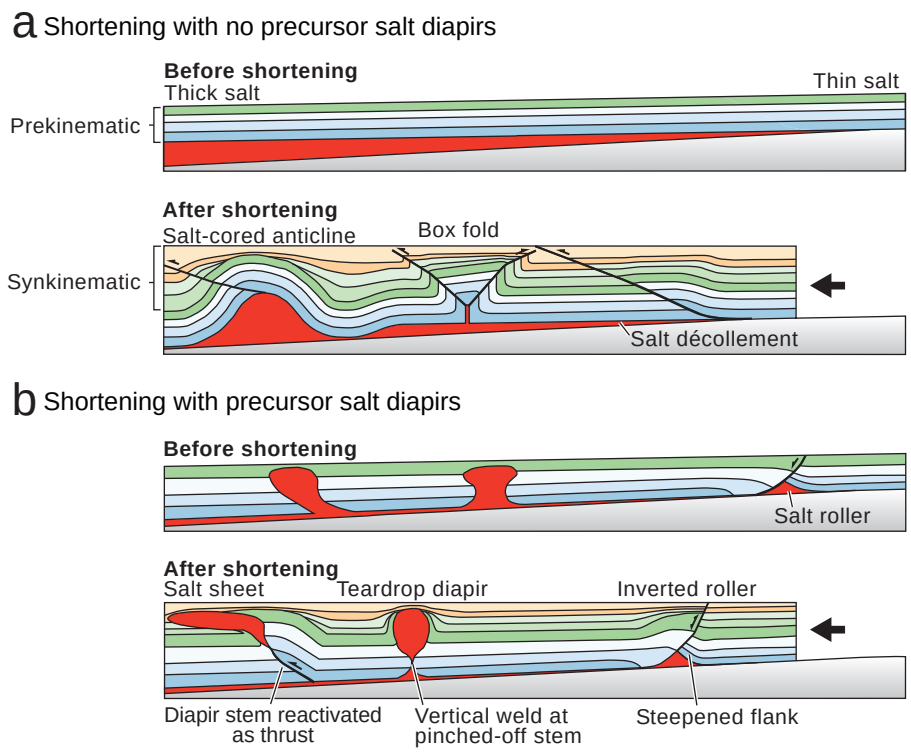
a Shortening with no precursor salt diapirs
Before shortening
Thick salt
Thin salt
Prekinematic
After shortening
Salt-cored anticline
Box fold
Synkinematic
Salt décollement
b Shortening with precursor salt diapirs
Before shortening
Salt roller
After shortening
Salt sheet
Teardrop diapir
Inverted roller
Diapir stem reactivated as thrust
Vertical weld at pinched-off stem
Steepened flank

Figure 1

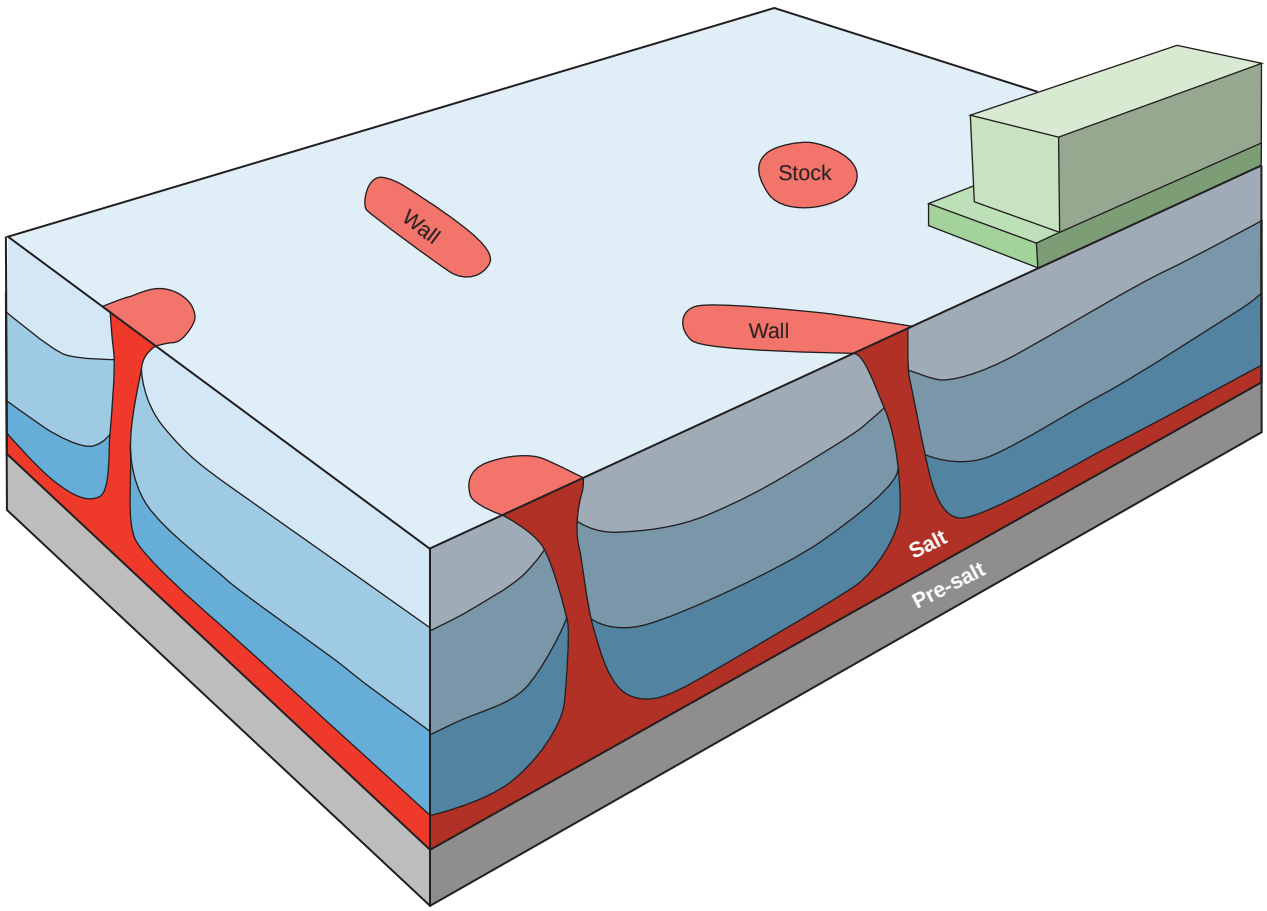

Figure 2

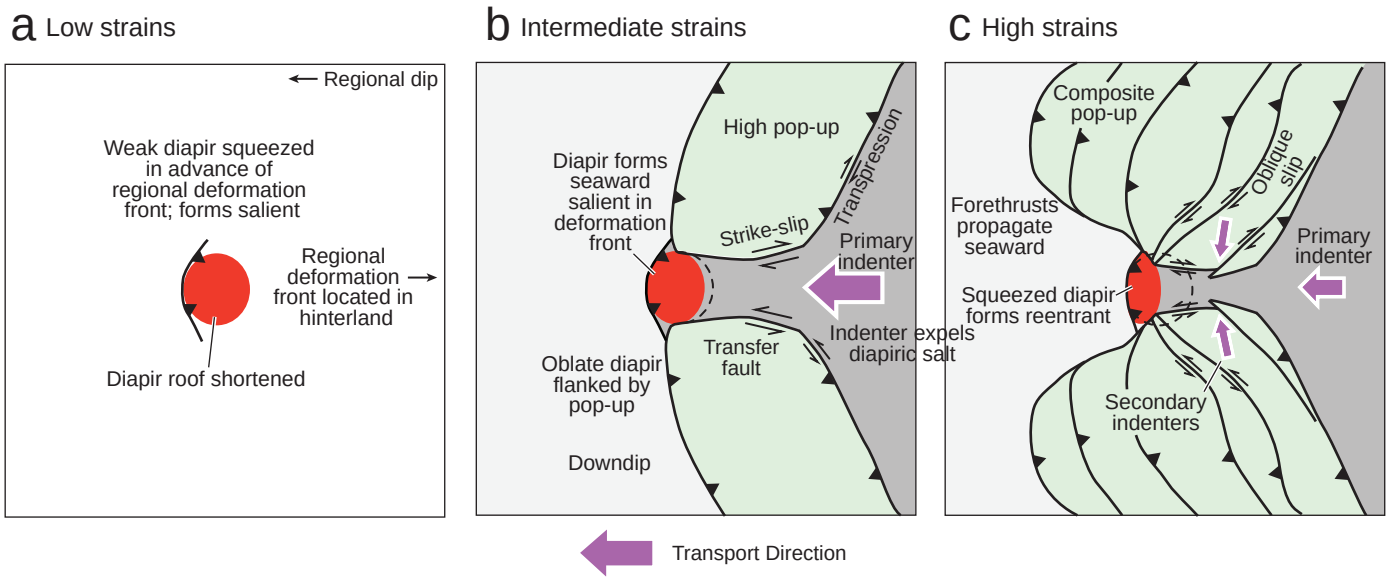
a Low strains
Regional dip
Weak diapir squeezed in advance of regional deformation front; forms salient
Regional deformation front located in hinterland
Diapir roof shortened
b Intermediate strains
High pop-up
Transpression
Diapir forms seaward salient in deformation front
Strike-slip
Primary indenter
Transfer fault
Indenter expels diapiric salt
Oblate diapir flanked by pop-up
Downdip
c High strains
Composite pop-up
Oblique slip
Forethrusts propagate seaward
Primary indenter
Squeezed diapir forms reentrant
Secondary indenters
Transport Direction

Figure 3

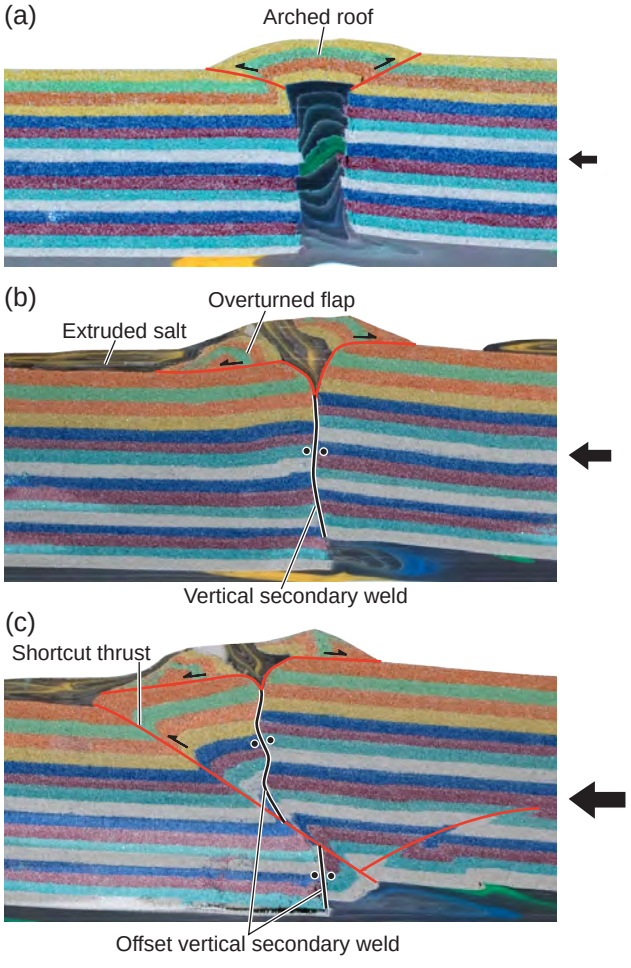
(a)
Arched roof
(b)
Overturned flap
Extruded salt
Vertical secondary weld
(c)
Shortcut thrust
Offset vertical secondary weld

Figure 4

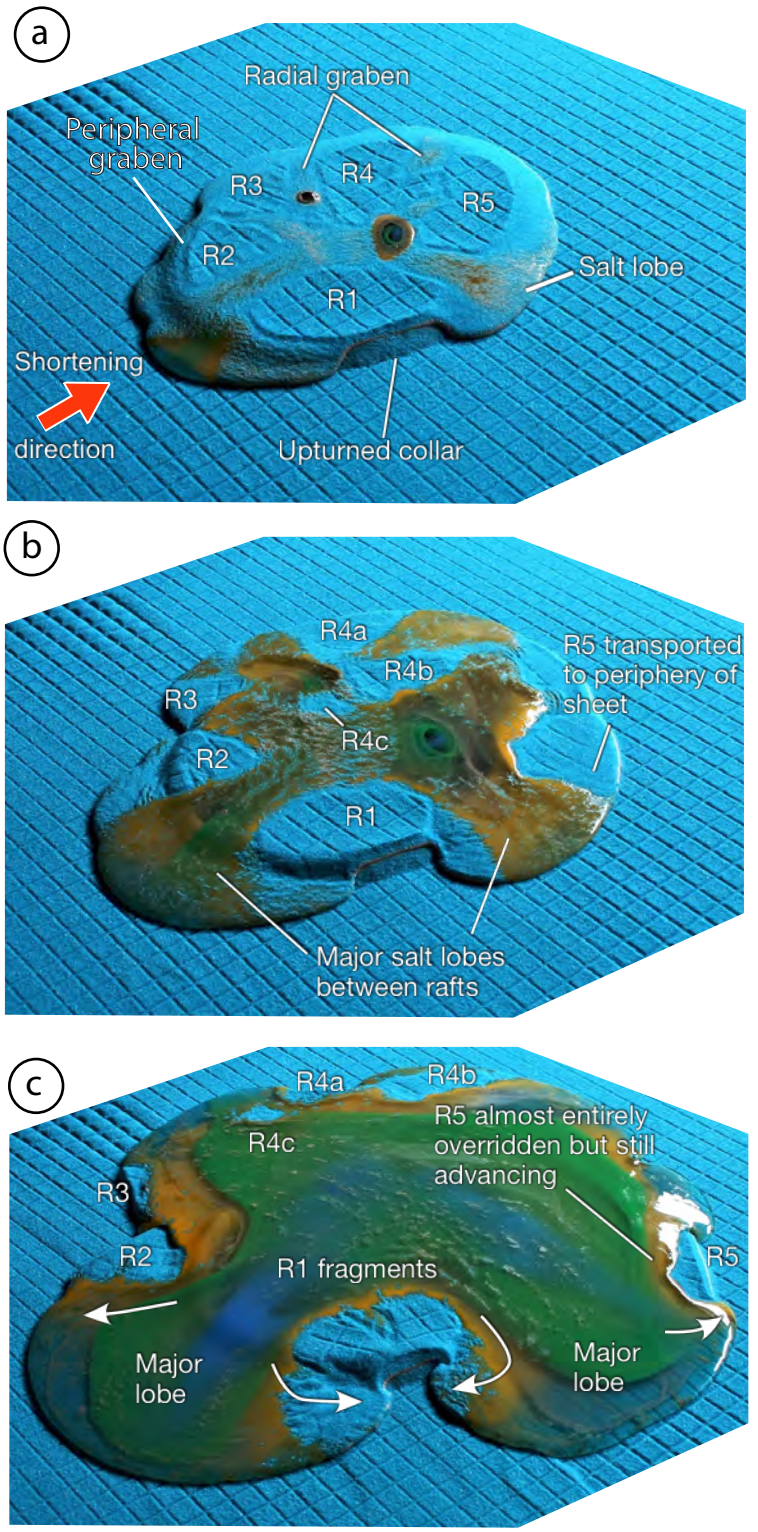
a
Radial graben
Peripheral graben
R3
R4
R5
R2
Salt lobe
R1
Shortening direction
Upturned collar
b
R4a
R4b
R5 transported to periphery of sheet
R3
R4c
R2
R1
Major salt lobes between rafts
c
R4a
R4b
R5 almost entirely overridden but still advancing
R4c
R3
R2
R1 fragments
R5
Major lobe
Major lobe

Figure 5

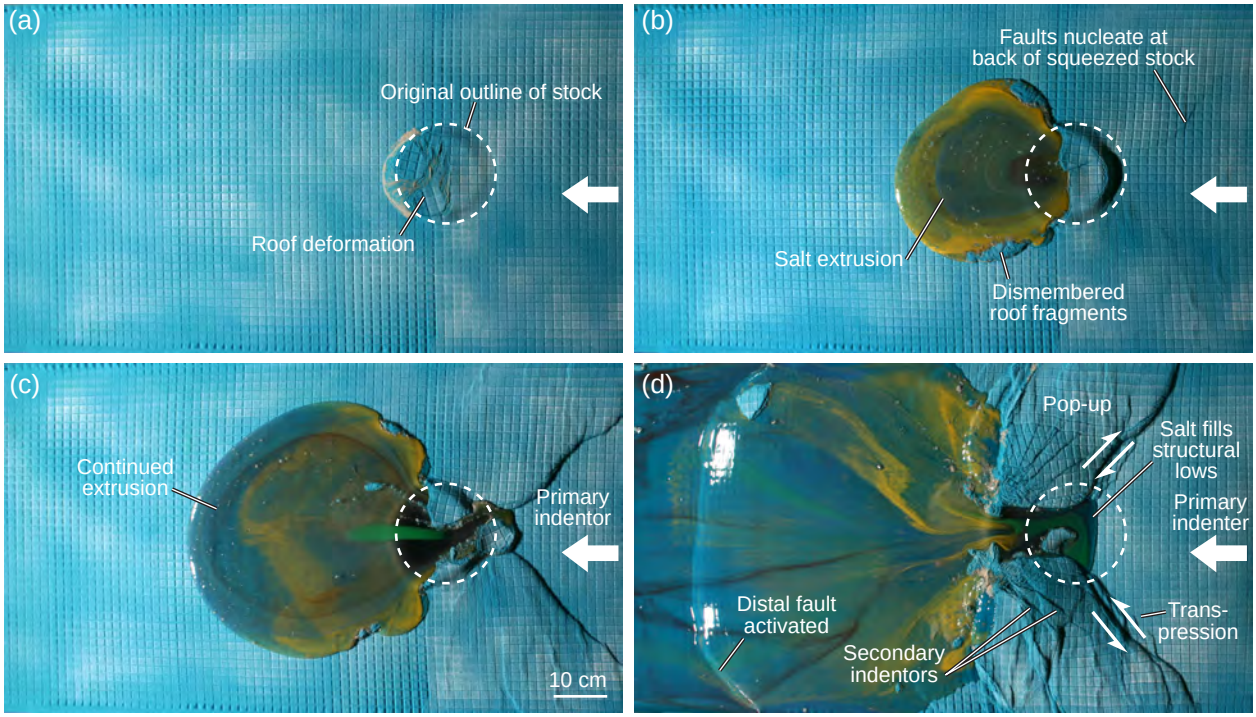
(a)
Original outline of stock
Roof deformation
(b)
Faults nucleate at
back of squeezed stock
Salt extrusion
Dismembered
roof fragments
(c)
Continued
extrusion
Primary
indentor
10 cm
(d)
Pop-up
Salt fills
structural
lows
Primary
indenter
Distal fault
activated
Secondary
indentors
Trans-
pression

Figure 6

Figure 7

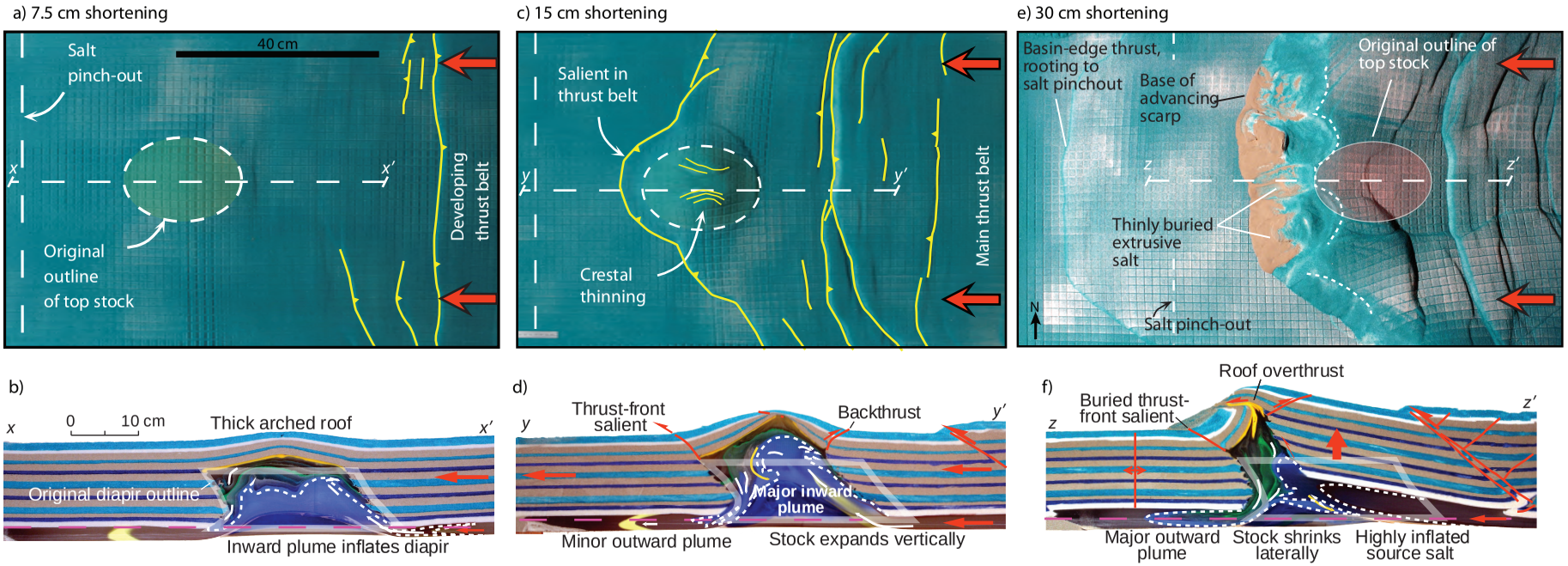
a) 7.5 cm shortening
40 cm
Salt pinch-out
x
x′
Original outline of top stock
Developing thrust belt
c) 15 cm shortening
Salient in thrust belt
y
y′
Crestal thinning
Main thrust belt
e) 30 cm shortening
Basin-edge thrust, rooting to salt pinchout
Base of advancing scarp
Original outline of top stock
z
z′
Thinly buried extrusive salt
N
Salt pinch-out
b)
x
0
10 cm
Thick arched roof
x′
Original diapir outline
Inward plume inflates diapir
d)
y
Thrust-front salient
Backthrust
y′
Major inward plume
Minor outward plume
Stock expands vertically
f)
Roof overthrust
Buried thrust-front salient
z
z′
Major outward plume
Stock shrinks laterally
Highly inflated source salt

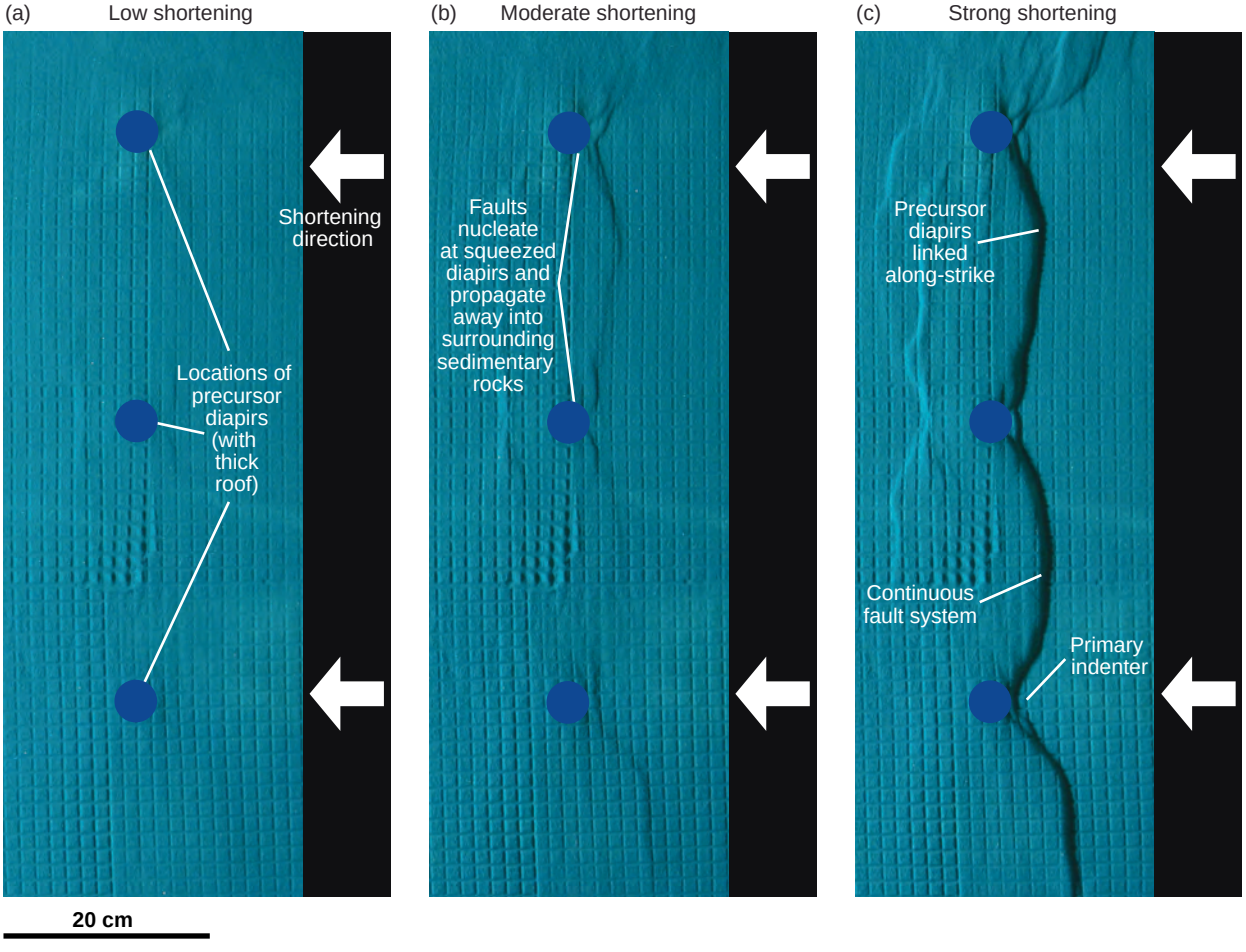
(a)
Low shortening
Shortening direction
Locations of precursor diapirs (with thick roof)
(b)
Moderate shortening
Faults nucleate at squeezed diapirs and propagate away into surrounding sedimentary rocks
(c)
Strong shortening
Precursor diapirs linked along-strike
Continuous fault system
Primary indenter
20 cm

Figure 8

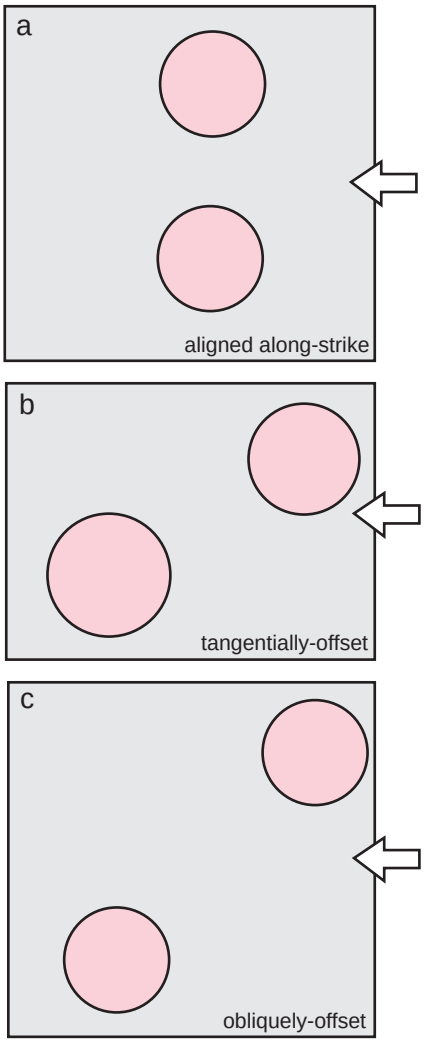
a
aligned along-strike
b
tangentially-offset
c
obliquely-offset

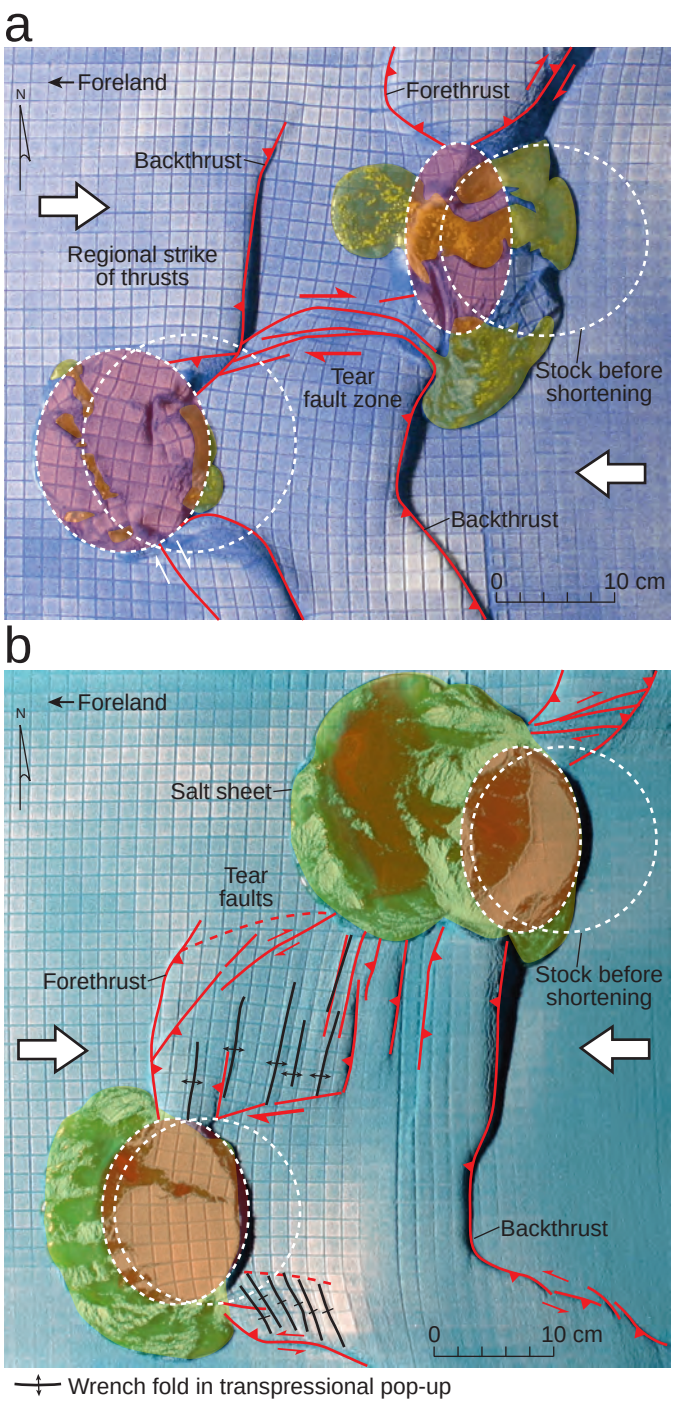
a
Foreland
N
Forethrust
Backthrust
Regional strike
of thrusts
Tear
fault zone
Stock before
shortening
Backthrust
0
10 cm
b
Foreland
N
Salt sheet
Tear
faults
Forethrust
Stock before
shortening
Backthrust
0
10 cm
Wrench fold in transpressional pop-up

Figure 10

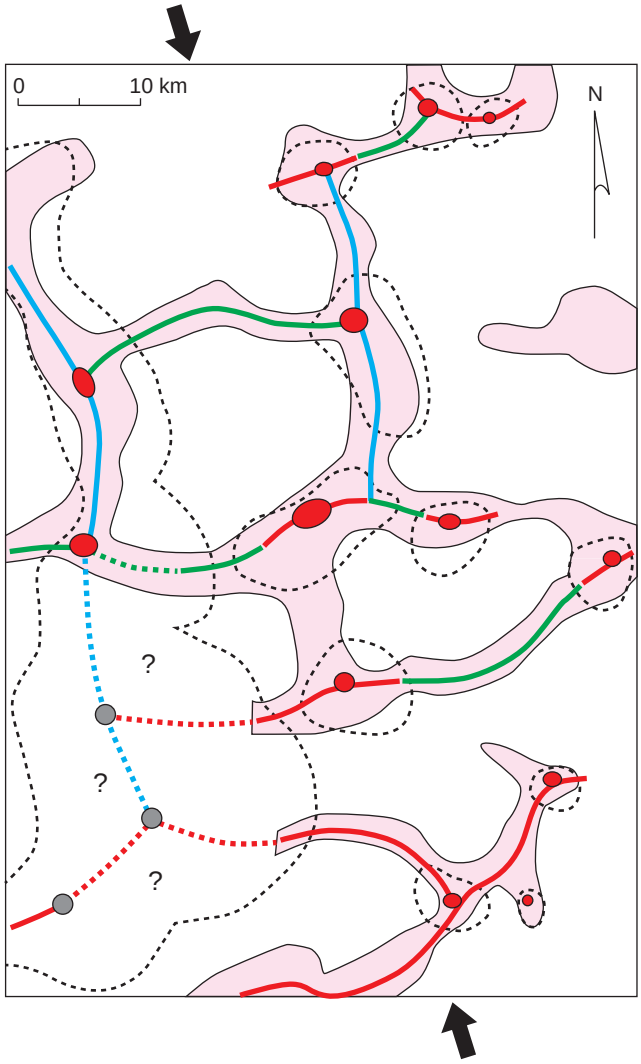

Figure 11

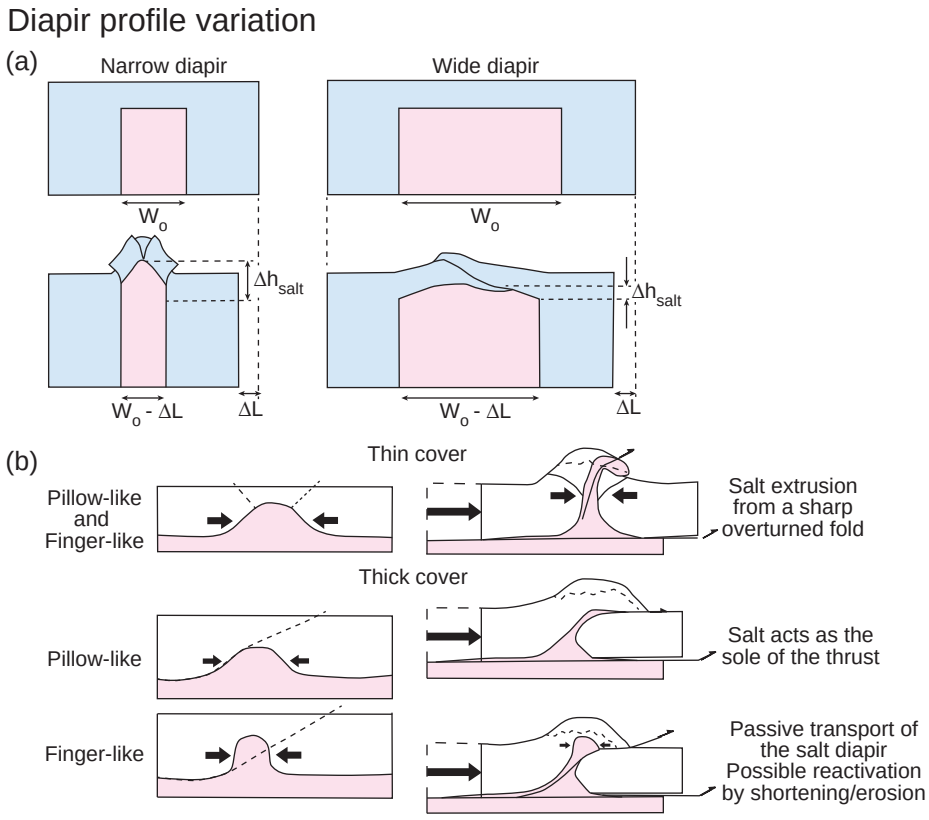
Diapir profile variation
(a)
Narrow diapir
Wide diapir
W o
W o
Δh salt
Δh salt
W o - ΔL
ΔL
W o - ΔL
ΔL
(b)
Thin cover
Pillow-like and Finger-like
Salt extrusion from a sharp overturned fold
Thick cover
Pillow-like
Salt acts as the sole of the thrust
Finger-like
Passive transport of the salt diapir
Possible reactivation by shortening/erosion

Figure 12a

Diapir planform variation

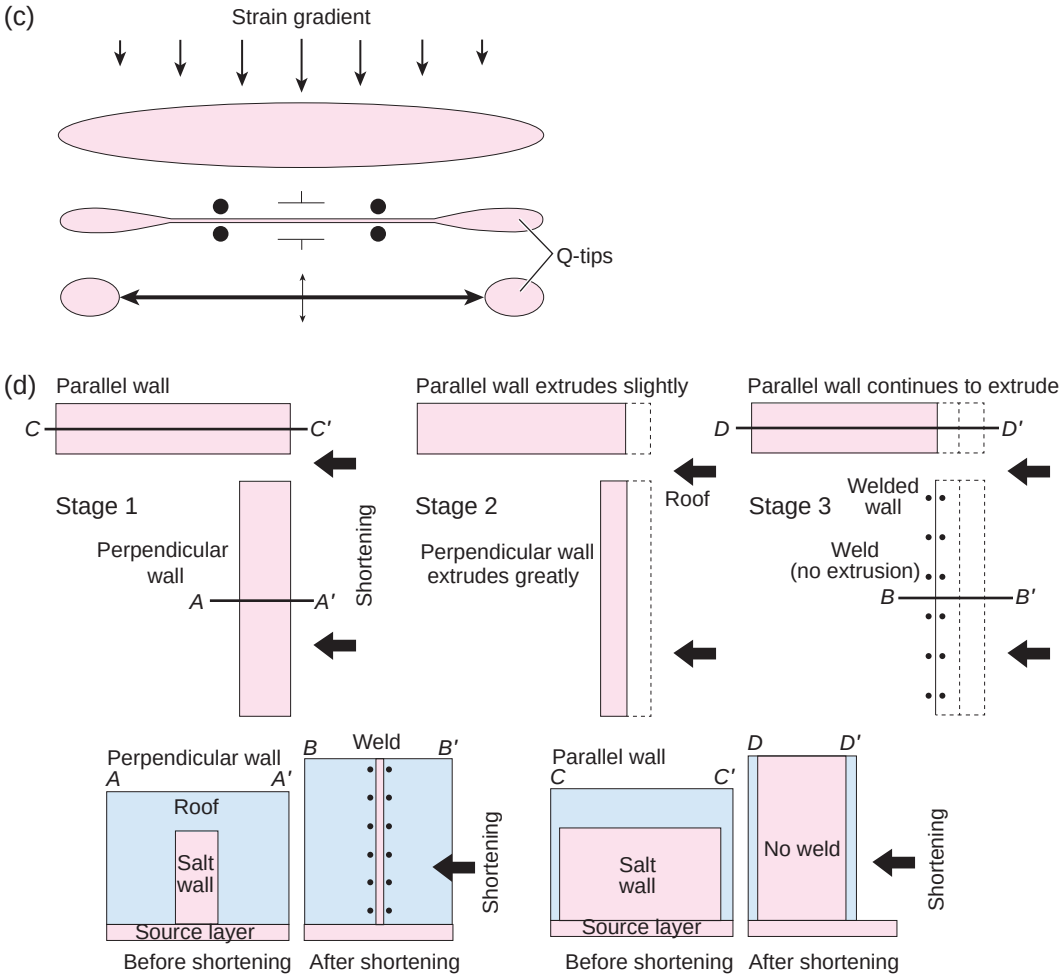

Figure 12b

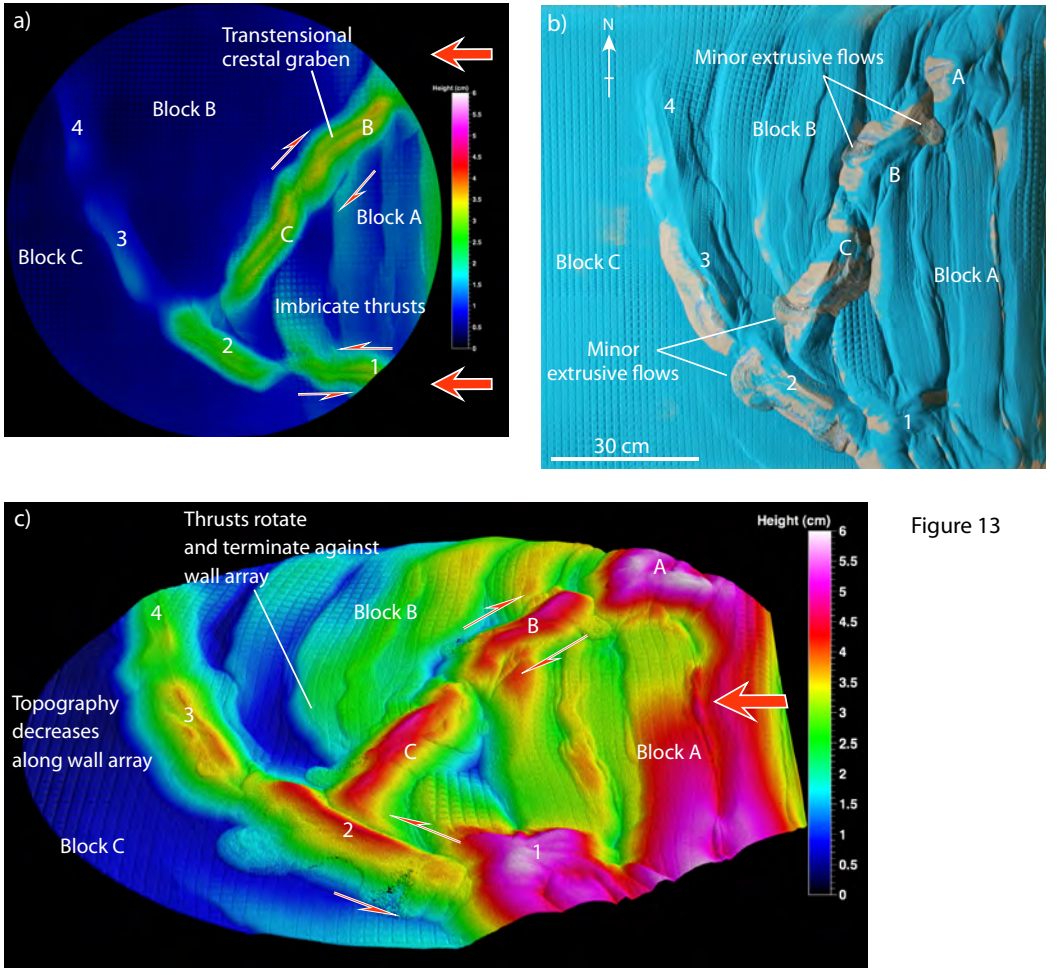
a)
Transtensional
crestal graben
Block B
4
B
Block A
C
3
Block C
Imbricate thrusts
2
1
b)
N
Minor extrusive flows
A
4
Block B
B
Block C
3
C
Block A
Minor
extrusive flows
2
1
30 cm
c)
Thrusts rotate
and terminate against
wall array
Height (cm)
6
5.5
5
4.5
4
3.5
3
2.5
2
1.5
1
0.5
0
A
4
Block B
B
Topography
decreases
along wall array
3
C
Block A
2
Block C
1

Figure 13

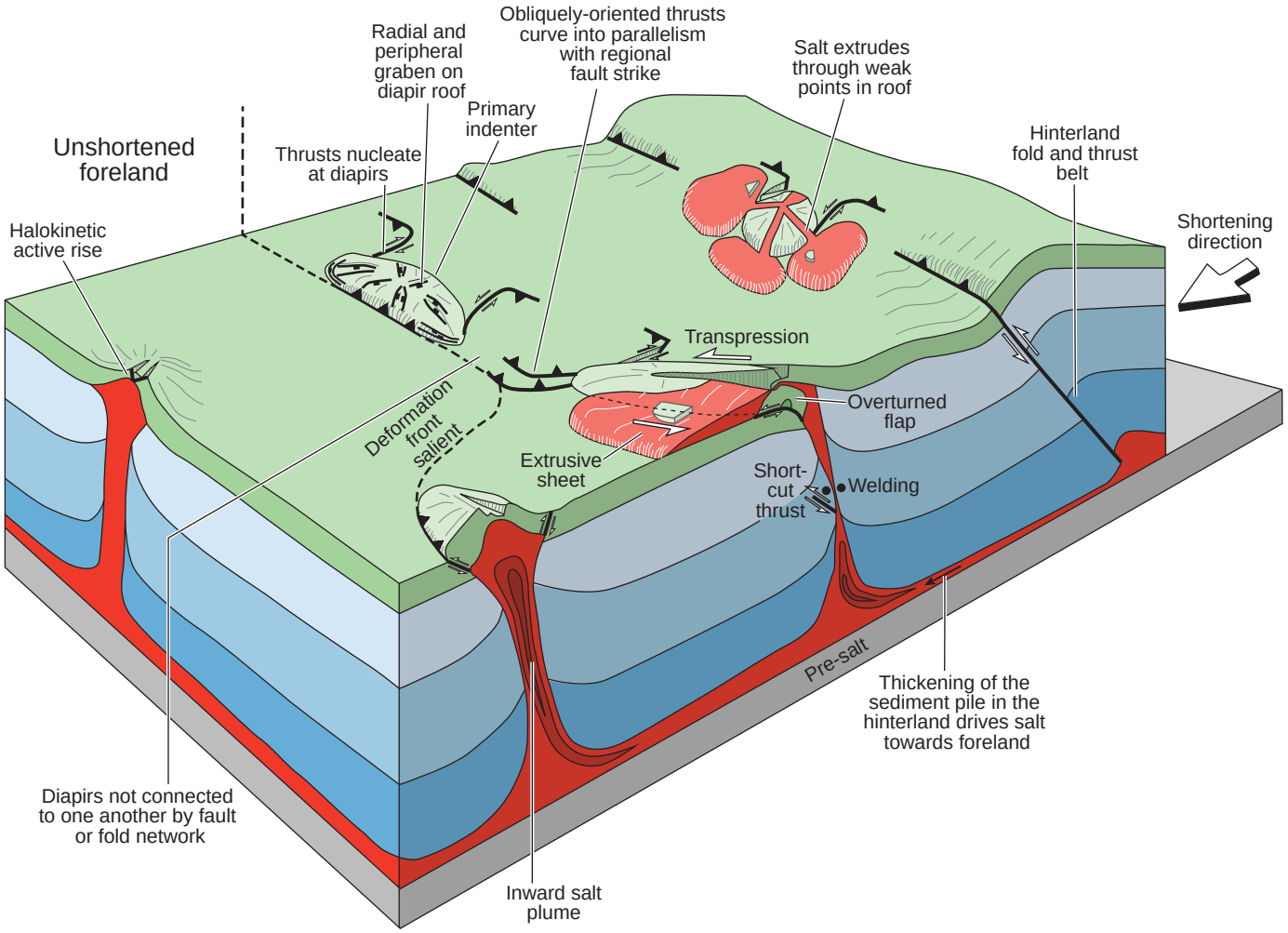
Unshortened foreland
Halokinetic active rise
Thrusts nucleate at diapirs
Radial and peripheral graben on diapir roof
Primary indenter
Obliquely-oriented thrusts curve into parallelism with regional fault strike
Salt extrudes through weak points in roof
Hinterland fold and thrust belt
Shortening direction
Transpression
Deformation front salient
Extrusive sheet
Overturned flap
Short-cut thrust
Welding
Pre-salt
Thickening of the sediment pile in the hinterland drives salt towards foreland
Diapirs not connected to one another by fault or fold network
Inward salt plume

Figure 14a

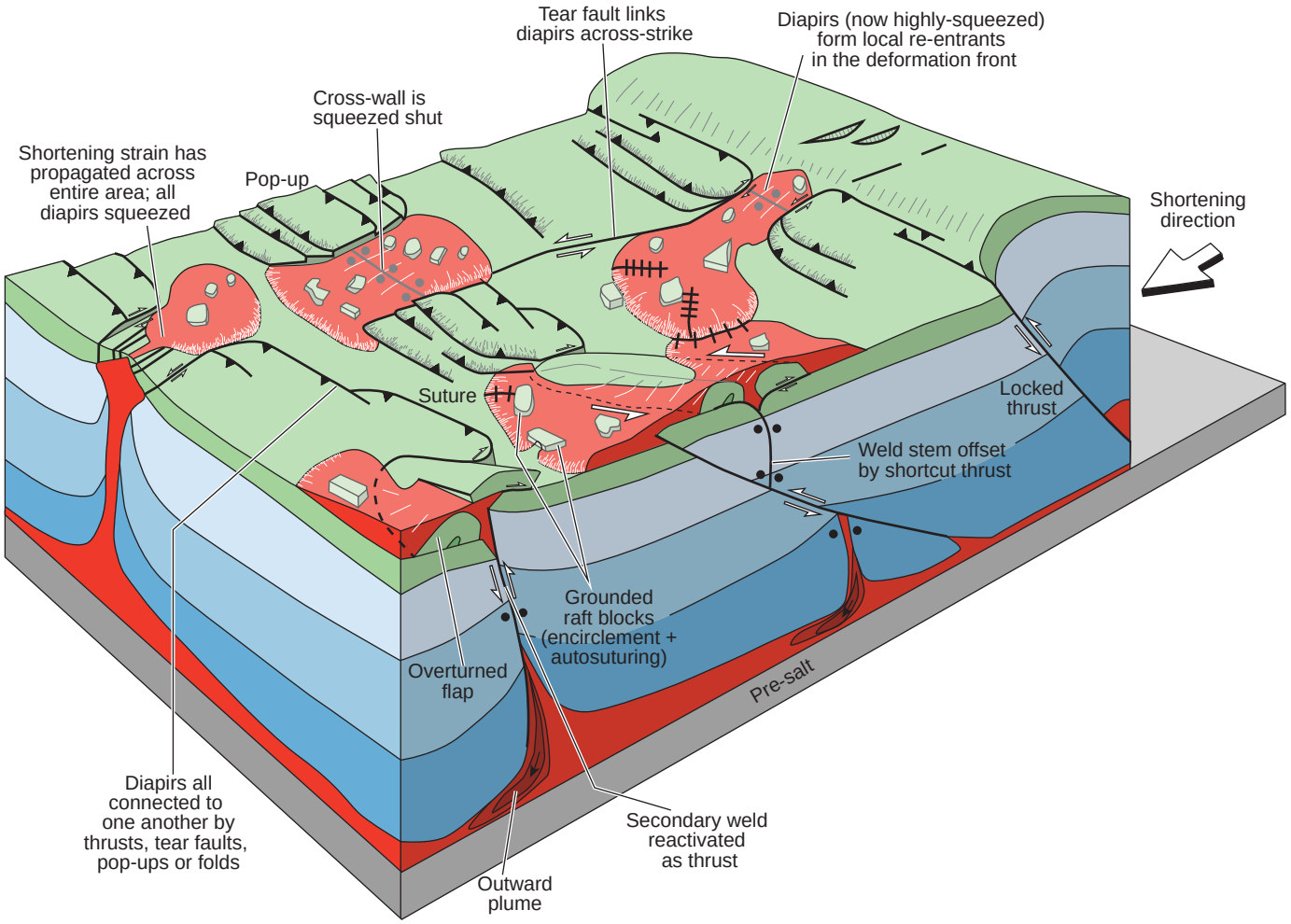
Tear fault links
diapirs across-strike
Diapirs (now highly-squeezed)
form local re-entrants
in the deformation front
Cross-wall is
squeezed shut
Shortening strain has
propagated across
entire area; all
diapirs squeezed
Pop-up
Shortening
direction
Suture
Locked
thrust
Weld stem offset
by shortcut thrust
Grounded
raft blocks
(encirclement +
autosuturing)
Overturned
flap
Pre-salt
Diapirs all
connected to
one another by
thrusts, tear faults,
pop-ups or folds
Secondary weld
reactivated
as thrust
Outward
plume

Figure 14b

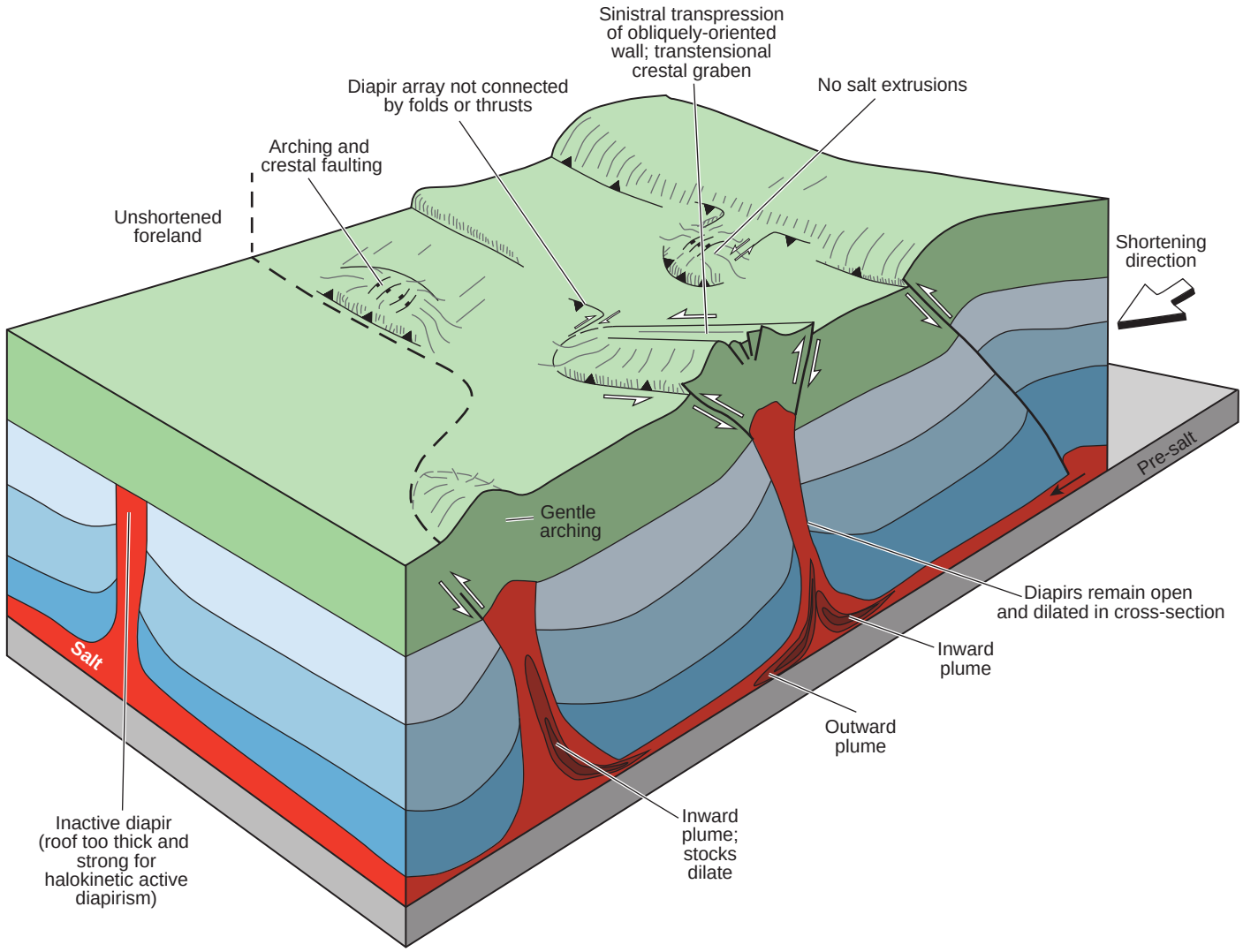
Sinistral transpression
of obliquely-oriented
wall; transtensional
crestal graben
Diapir array not connected
by folds or thrusts
No salt extrusions
Arching and
crestal faulting
Unshortened
foreland
Shortening
direction
Gentle
arching
Pre-salt
Diapirs remain open
and dilated in cross-section
Inward
plume
Outward
plume
Salt
Inactive diapir
(roof too thick and
strong for
halokinetic active
diapirism)
Inward
plume;
stocks
dilate

Figure 15a

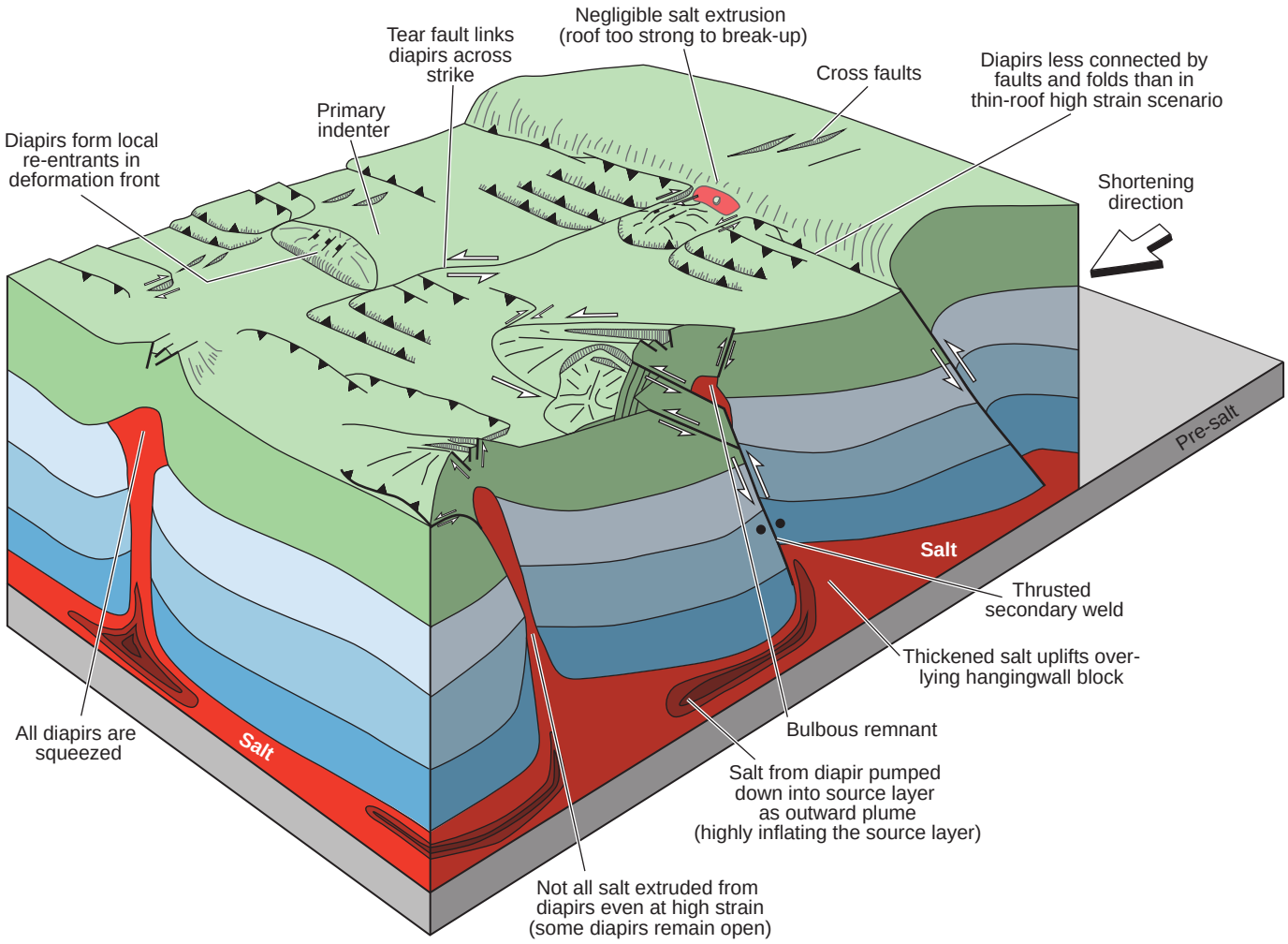
Negligible salt extrusion
(roof too strong to break-up)
Tear fault links
diapirs across
strike
Cross faults
Diapirs less connected by
faults and folds than in
thin-roof high strain scenario
Primary
indenter
Diapirs form local
re-entrants in
deformation front
Shortening
direction
Pre-salt
Salt
Thrusted
secondary weld
Thickened salt uplifts over-
lying hangingwall block
All diapirs are
squeezed
Salt
Bulbous remnant
Salt from diapir pumped
down into source layer
as outward plume
(highly inflating the source layer)
Not all salt extruded from
diapirs even at high strain
(some diapirs remain open)

Figure 15b

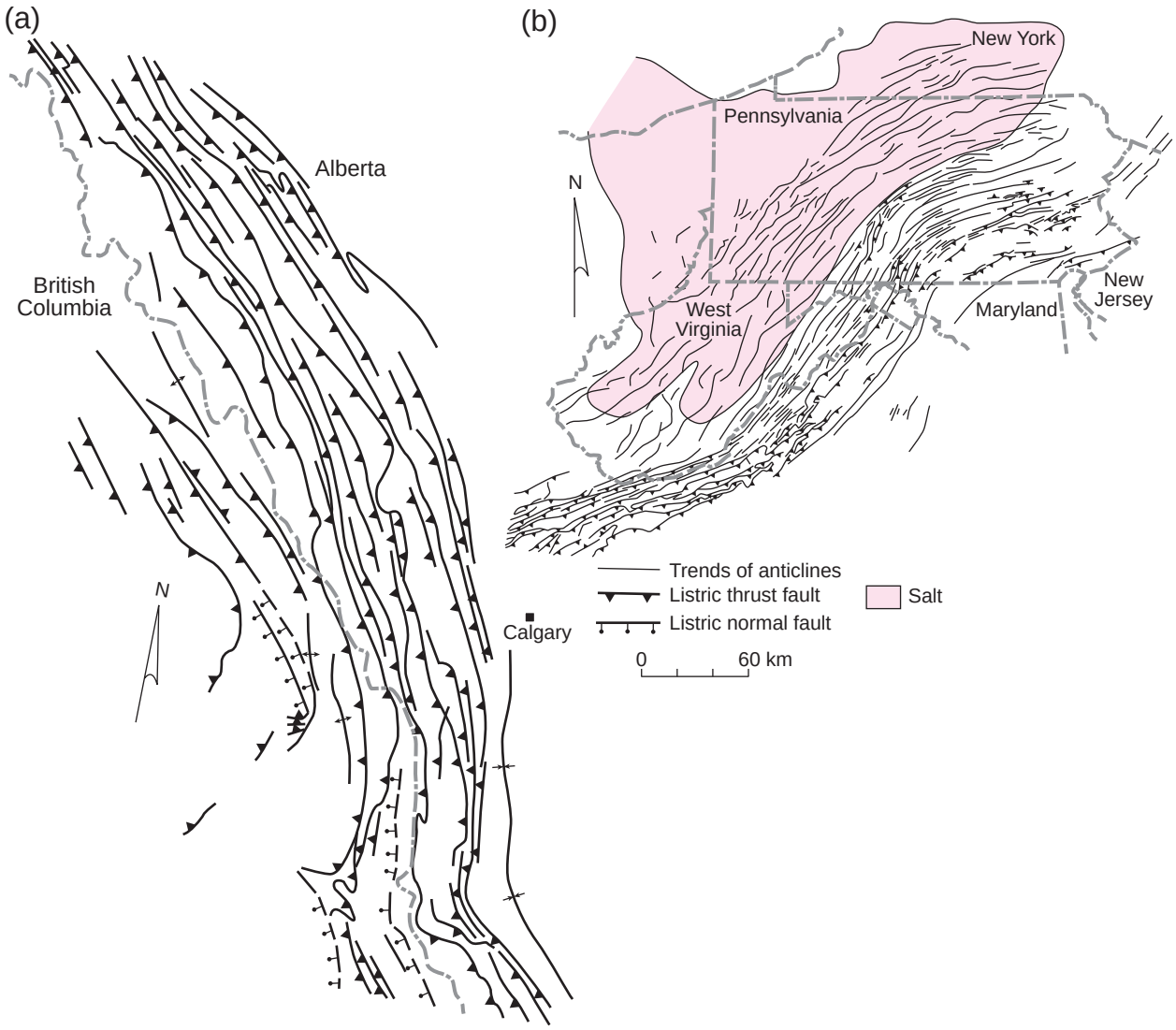
(a)
Alberta
British
Columbia
N
Calgary
(b)
New York
Pennsylvania
N
West
Virginia
Maryland
New
Jersey
Trends of anticlines
Listric thrust fault
Listric normal fault
Salt
0
60 km

Figure 16

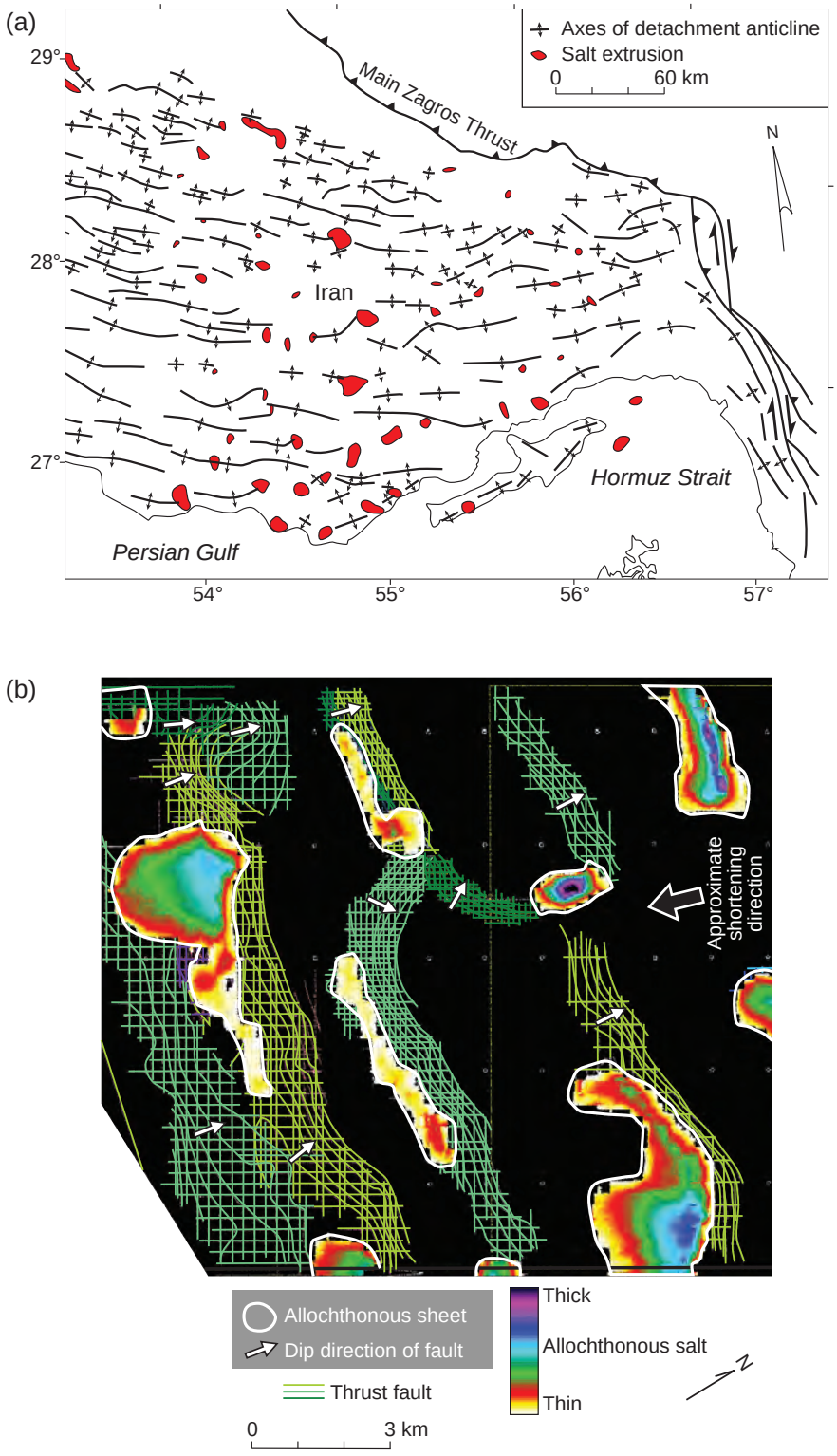
(a)
Axes of detachment anticline
Salt extrusion
0
60 km
Main Zagros Thrust
N
29°
28°
27°
Iran
Hormuz Strait
Persian Gulf
54°
55°
56°
57°
(b)
Approximate shortening direction
Allochthonous sheet
Dip direction of fault
Thrust fault
0
3 km
Thick
Allochthonous salt
Thin
N

Figure 17